

Master Thesis // Scarlett Sett

**The combined effect of
global warming and ocean acidification
on the coccolithophore
Gephyrocapsa oceanica
carbon production and physiology**

Advisor // Prof. Dr. Ulf Riebesell

Supervisor // Dr. Kai Schulz

Kiel, August 11th, 2010

A mis papas: Rolando y Margarita

TABLE OF CONTENTS	I-III
Abbreviations	IV
Figures	V
Tables	VI
Equations	VI
 Abstract	 VII
 1. INTRODUCTION	 1-9
1.1 Climate Change	1
1.2 Global Warming	1
Temperature and $p\text{CO}_2$ through time	1
Changes in ocean surface temperature and its effects	3
1.3 Seawater carbonate system and ocean acidification	3
Seawater carbonate system	3
Ocean acidification	5
1.4 Coccolithophores and biogeochemical element cycles	6
Coccolithophores	6
Importance of coccolithophores in biogeochemical element cycles	6
1.5 Significance and objectives of this study	8
 2. Materials and Methods	 10
2.1 Experimental setup	10
2.2 Coccolithophore culture and media	11
2.3 Experimental parameters	12
2.4 Sampling and Measurements	12
Dissolved inorganic carbon (DIC)	13
Total alkalinity (TA)	13
Total particulate carbon and nitrogen (TPC/TPN)	14
Particulate organic carbon and nitrogen (POC/PON)	14
Particulate inorganic carbon (PIC)	14

Particulate organic phosphorous (POP).....	15
Chlorophyll a (Chl a)	15
Cell densities and growth rate (μ)	15
Nutrients	15
Scanning electron microscopy (SEM)	16
2.5 Statistics	16
3. Results	17-26
3.1 Carbonate system.....	17
3.2 Growth rates	18
3.3 Cell quotas.....	19
Chlorophyll a cell quotas	19
POC cell quotas	19
PIC cell quotas.....	19
3.4 Production rates.....	21
Chlorophyll a production rates	21
POC production rates	21
PIC production rates	21
3.5 Ratios	23
POC:PON ratios.....	23
PIC:POC ratios	23
3.6 SEM images	25
4. Discussion	27-35
4.1 Growth rates	27
4.2 Particulate organic carbon production (POC)	29
4.3 Particulate inorganic carbon production rates.....	30
4.4 Element ratios (PIC:POC).....	33
4.5 Comparison to other coccolithophores	34
4.6 Summary and future perspectives	35

Appendix.....	36-43
AI. Carbonate system	36
AII. 20°C Carbonate system, cellular contents and p roduction rates	37
AIII. 15°C Carbonate system, cellular contents and production rates	38
AIV. Carbonate system parameters (from measured TA and DIC averages)	39
AV. Nutrient concentrations at beginning and end of experiment	40
AVI. POP and PON content and production rates	41
Literature	42
Acknowledgments	50

ASW	artificial seawater
Chl <i>a</i>	chlorophyll <i>a</i>
CO ₃ ²⁻	carbonate
CO ₂ [*]	term representing H ₂ CO ₃ [*] and CO ₂ (aq)
DIC	dissolved inorganic carbon
HCl	hydrochloric acid
HCO ₃ ⁻	bicarbonate
H ₂ CO ₃	carbonic acid
Na ₂ CO ₃	sodium carbonate
NSW	natural seawater
<i>p</i> CO ₂	partial pressure of CO ₂
PIC	particulate inorganic carbon
POC	particulate organic carbon
PON	particulate organic nitrogen
SEM	scanning electron microscope
SST	sea surface temperature
TA	total alkalinity
TPC	total particulate carbon
TPN	total particulate nitrogen

- Figure 1 Variation in CO₂ and temperature of the past 400,000 yrs
- Figure 2 Bjerrum plot
- Figure 3 Experimental setup
- Figure 4 Filtration system
- Figure 5 Growth rate as a function of $p\text{CO}_2$
- Figure 6a Cellular Chl a quotas
- Figure 6b Cellular POC quotas
- Figure 6c Cellular PIC quotas
- Figure 7a Chl a production rates
- Figure 7b POC production rates
- Figure 7c Calcification rates
- Figure 8a POC:PON ratio
- Figure 8b PIC:POC ratio
- Figure 9 SEM images at 15°C
- Figure 10 SEM images at 20°C
- Figure 11 SEM image comparison between 15 and 20°C
- Figure 12 Growth rate as a function of temperature
- Figure 13 Growth rate as a function of $p\text{CO}_2$
- Figure 14 POC production as a function of $p\text{CO}_2$
- Figure 15 Calcification rates as a function of $p\text{CO}_2$
- Figure 16 PIC quotas as a function of $p\text{CO}_2$
- Figure 17 PIC:POC comparison

Table 1	Experimental carbonate system
Table 2	Statistical summary for production rates
Table 3	Comparison of culture incubation conditions
Table 4	Comparison of strains and incubation conditions
Equation 1	Carbonate system equilibrium equations
Equation 2	Sum of dissolved inorganic carbon species
Equation 3	Simplified total alkalinity equation
Equation 4	Calcification equation
Equation 5	Photoyynthesis equation
Equation 6	PIC equation
Equation 7	Chlorophyll <i>a</i> equation
Equation 8	Growth rate equation
Equation 9	TPC buildup equation
Equation 10	Non-linear regression equation used for data fitting

Abstract

Climate change is expected to impact oceanic ecosystem functioning in the upcoming decades, ocean acidification and global warming being the most important factors which will shape the future ocean dynamics (Jackson 2008). In the experiments presented here we used an innovative approach that consisted of extending the number of treatments across a wide range of carbon dioxide partial pressure ($p\text{CO}_2$) levels and two temperatures which allowed to test lower and upper thresholds of biological production. Growth, calcification and POC production rates showed an optimum curve response to increasing $p\text{CO}_2$, with an almost doubling in production rates at 20°C and optimum rates for $p\text{CO}_2$ levels of ~290-599 μatm at 15°C and ~488-1052 μatm $p\text{CO}_2$ at 20°C. PIC and POC cellular quotas showed changes to increasing $p\text{CO}_2$ but no effect from increasing temperature. Results obtained from the combined effect of global warming and increasing $p\text{CO}_2$ from these experiments might contribute to shape biogeochemical modeling formulations in the near future.

1. INTRODUCTION

1.1 Climate change

The oceans occupy about 71% of the Earth's surface and play a significant role in sustaining life on Earth. Increasing atmospheric CO₂ has been directly linked to human activity since the beginning of the industrial revolution (Sabine et al. 2004) and climate change is expected to impact oceanic ecosystem functioning and services in the upcoming decades, ocean acidification and global warming being the most important factors that will shape future ocean dynamics (Jackson 2008). The rapid increase in atmospheric CO₂ has been buffered by the ability of the ocean to absorb and sequester CO₂. The term "ocean acidification" has been coined to describe the decrease in carbonate [CO₃²⁻] ions, increase in bicarbonate [HCO₃⁻] ions, overall increase in DIC and decrease in pH (Caldeira and Wickett 2003). On the other hand, according to model predictions, changes in ocean surface temperatures will further reduce CO₂ uptake capacity by decreasing CO₂ solubility in the ocean (Maier-Reimer et al. 1996; Barker et al. 2003). Evidence suggests that the second half of the 20th century showed the highest recorded average temperatures in the past 50 years (IPCC 2007). The impact of increasing temperature in the ocean could range from changes in phytoplankton assemblages (Wohlers et al. 2009) to individual growth rates (Buitenhuis et al. 2008), and export production (Buesseler et al. 2007). It is crucial to study the responses of ocean biogeochemistry and its feedbacks in the future perspective of "a high CO₂ and warmer ocean" taking into consideration interactions of environmental parameters (Sarmiento et. al. 2004, Rost et al. 2008).

1.2 Global warming

Temperature and pCO₂ over time

In order to symbolize the heat capacity of the ocean versus the atmosphere, it is estimated that for every 0.1°C increase in ocean temperature there would be a 100°C increase in global atmosphere temperature (this would be possible in a

scenario in which heat was transferred directly from the ocean to the atmosphere) (Levitus et al. 2005). It is important to note that most significant increases in ocean temperatures occur above 700 meters (Levitus et al. 2005) since the ocean's interior is relatively constant in terms of environmental parameters (Gage and Tyler 1991). Any temperature change is thus relevant for phytoplankton inhabiting the euphotic zone. The surface ocean temperature is an easily measured, obvious variable for which there are century-long records in the oceans and which will change significantly as a consequence of climate change (Kleypas et al. 2001). So far, increasing temperature has shown a direct correlation to increasing atmospheric CO₂ on longer time scales, but it is not clear which parameter dominates/triggers the other (Figure 1). For our present situation it is clear that increasing atmospheric CO₂ is leading to a general increase in temperature.

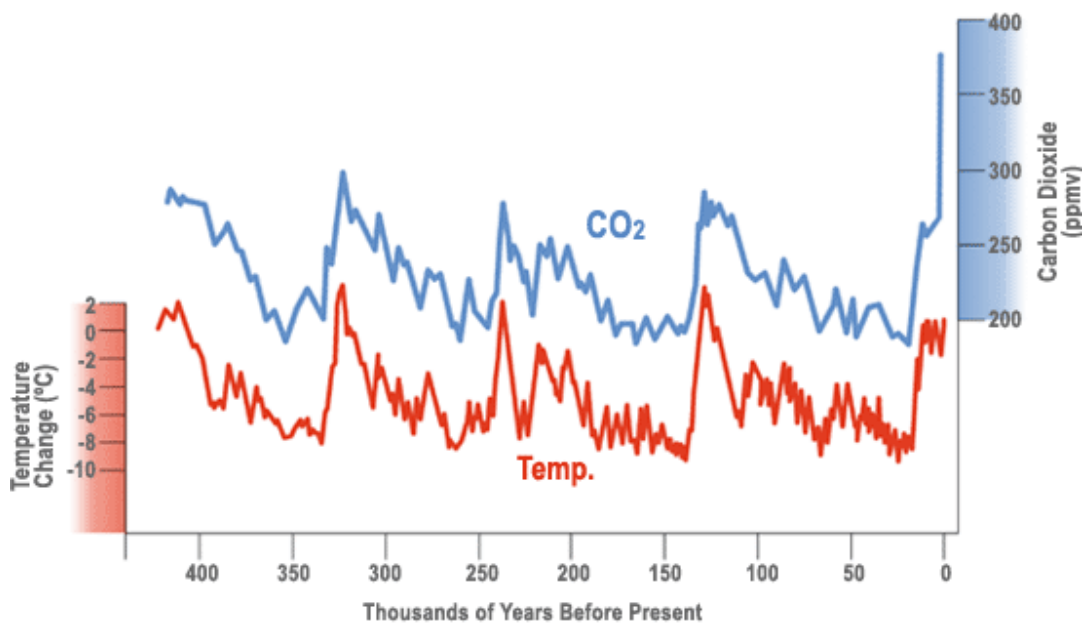


Figure 1. CO₂ concentrations (p.p.m.v.) plotted against atmospheric temperature change derived from isotopic oxygen profile in the Vostok ice core record (Petit et al. 1999)

Changes in ocean surface temperatures and its possible effects

Warming of the oceans, referred to an increase in sea surface temperature (SST), is prevalent in all oceans and more intense in higher latitudes (IPCC 2007). Temperature changes can be connected to physicochemical properties such as vertical stratification and nutrient availability (Carder et al. 1999; Sathyendranath et al. 2001). These parameters (e.g. temperature changes, nutrient availability and vertical stratification) are thought to be the main driver of seasonal and regional changes (Bouman et al. 2003) in phytoplankton community assemblages. In Northern latitudes, where phytoplankton is limited by light availability and not by nutrients, a stronger stratification would allow for possible increases in productivity. Meanwhile, in the tropics and mid latitude regions, phytoplankton is usually limited by nutrient concentrations and depend strongly on deep mixing to bring deep nutrient-rich waters to surface. Therefore stronger stratification would not allow for this deep-mixing process to happen (reducing the strength) and a decrease in productivity would be more likely (Riebesell et al. 2009). A reduction of 9-15% of CO₂ uptake capacity by the oceans due to warming is expected by the end of the 21st century (Sarmiento and LeQuere 1996; Joos et al. 1999; Matebr and Hirst 1999; Plattner et al. 2003). In addition to global warming as a consequence of increasing atmospheric CO₂, there is also the “other CO₂ problem”: ocean acidification (Doney et al. 2009).

1.3 Seawater carbonate system and ocean acidification

Seawater Carbonate system

The seawater carbonate system is composed of four measurable parameters, from which any two are sufficient to calculate the others given temperature, salinity and pressure (Sarmiento and Gruber 2006). These four parameters are dissolved inorganic carbon (DIC), total alkalinity (TA), pH and CO₂ partial pressure (pCO₂). DIC and TA are preferably used because they are considered conservative quantities with respect to changes in state and will be the only ones described here.

When atmospheric CO_2 dissolves in seawater, it reacts with water (H_2O) to form carbonic acid (H_2CO_3) which then dissociates into bicarbonate (HCO_3^-) and carbonate (CO_3^{2-}) according to the following reactions:



Since $\text{CO}_2(\text{aq})$ and H_2CO_3 are not easily distinguished, they are clumped into a new term called CO_2^* . DIC represents the pool of dissolved inorganic carbon in the ocean and it is composed of the sum of all dissolved species. DIC speciation in the ocean is defined as:

$$\text{DIC} = [\text{CO}_2^*] + [\text{HCO}_3^-] + [\text{CO}_3^{2-}] \quad (\text{equation 2})$$

The three different species, CO_2^* , HCO_3^- and CO_3^{2-} , are found in seawater at different concentrations (>1%, ~90% and ~9%, respectively at typical surface ocean pH of 8.1) as a function of pH (Wolf-Gladrow et al. 1999) according to Figure 2:

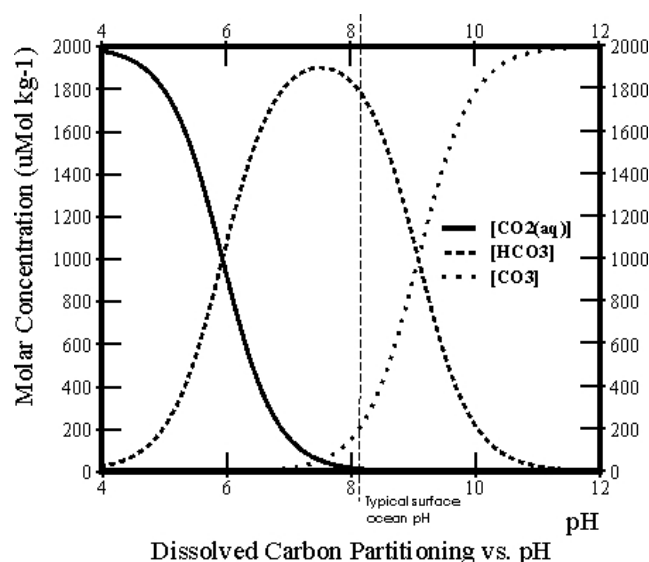


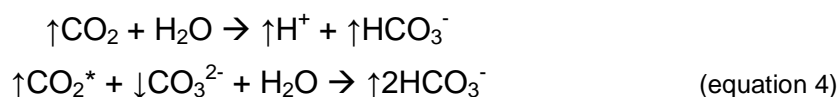
Figure 2. Bjerrum plot with concentrations of dissolved inorganic carbon species (CO_2^* , HCO_3^- and CO_3^{2-}) as a function of pH. At 15°C and salinity of 35.

Another important key parameter from the carbonate system is TA. TA has different definitions depending on chemical or physical perspectives and it can be regarded as the natural buffer of the ocean. Chemically it is defined as measured by titration with a strong acid (Dickson 2007), while physically it is defined as the charge balance of ions (Wolf-Gladrow et al. 2007). Regardless of the preferred definition, for simplicity we will define TA simply as carbonate alkalinity:

$$TA = [HCO_3^-] + 2[CO_3^{2-}] \quad (\text{equation 3})$$

Ocean acidification

Presently, the ocean takes up more than 1/3 of the anthropogenic CO₂ emissions, partially mitigating the effect of climate warming but changing ocean carbonate chemistry balance (Orr et al. 2005). As atmospheric CO₂ increases there is also an increase in dissolved CO₂ in the ocean, leading to a shift in DIC speciation. This shift lowers the buffering capacity of the ocean which is thought to be associated to the [CO₃²⁻] ion ability to react with excess CO₂ from the atmosphere (Riebesell et al. 2009) through the following reactions:



As seawater pCO₂ continues to rise along atmospheric CO₂ concentrations it is estimated that a 30% reduction in [CO₃²⁻] and a 60% increase in [H⁺] would likely occur leading to a diminishing effect on the ocean's ability to sequester atmospheric CO₂ (Sabine et al. 2004). Additionally, ocean water pH is expected to decrease about 0.4 units by the end of the century assuming estimations of the IPCC "business as usual" scenario (Wolf-Gladrow et al. 1999).

1.4 Coccolithophores and biogeochemical cycles

Coccolithophores

Coccolithophores are single-cell, autotrophic algae which belong to the phylum Haptophyta and class of Prymnesiophyceae. They are ubiquitously spread in the world oceans but the ones that live in boreal waters are extremely abundant (McIntyre and Be 1967). These high latitude species are important because of their ability to produce intensive blooms which extend for hundredths of kilometers and which are detectable from space (e.g. Holligan et al. 1983, 1993; Groom and Holligan 1987; Balch et al. 1991, 1996; Tyrell et al. 1996). The only two bloom-forming coccolithophore species are *Emiliania huxleyi* (Balch et al. 1992; Winter et al. 1994; Broerse et al. 2003) and *G. oceanica*. *G. oceanica* has shown to be more sensitive to changes in seawater carbonate chemistry in terms of decrease calcification and increase POC production on a range of pre-industrial to estimated year 2100 $p\text{CO}_2$ levels (Riebesell et al. 2000; Zondervan et al. 2001). Many coccolithophores including *G. oceanica* also produce alkenones which serve as proxies for temperature in ocean surface water (Prahl 1988; Jasper 1990, 1994; Conte et al. 1998; Stoll and Ziveri 2004) and have fossil records worldwide if above the carbonate compensation depth or CCD (Stoll et al. 2002). It was also suggested by McIntyre (1970) that *E. huxleyi* had evolved from two *Gephyrocapsa* spp. groups, according to morphological characteristics. The presence of *G. oceanica* in sedimentary records, and its production of alkenones, dates back 45 million years compared to records from *E. huxleyi* of only 265,000 years (Volkman et al. 1995).

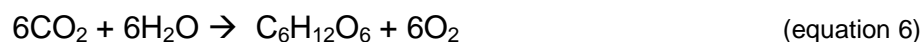
Importance of coccolithophores in biogeochemical cycles

Coccolithophores are important model organisms because they represent a significant part of the marine food web (Bollman and Klaas 2008) as the most important calcareous primary producers as well as significant players in global biogeochemical cycles (Balch et al. 2007; Bollman and Klaas 2008). They are one of the calcifying groups [the other being pteropods (Gangsto et al. 2008)]

implemented in global biogeochemical models representing pelagic calcification in the oceans (Gehlen et al. 2007). Coccolithophores play an important role in the marine carbon cycle because they directly participate in both biological carbon pumps (calcium carbonate and soft tissue pump) (Klaas and Archer 2002). In the process of calcification (calcium carbonate pump) they change DIC and TA in a 1:2 ratio, respectively (Wolf-Gladrow et al. 1999) and potentially act as a source of CO₂ (Frankignoulle et al. 1994; Buitenhuis et al. 2001; Zondervan et al. 2001). CO₂ released in the process of calcification increases as a function of increasing pCO₂ (Frankignoulle et al. 1994) and can be thought to be released according to the following equation:



On the other hand, CO₂ (eventually released from calcification) is used in photosynthesis. Whether there is a net uptake/release of CO₂ by coccolithophores depends on the ratio of photosynthesis to calcification or the so called PIC:POC. CO₂ is used to drive photosynthesis according to the following:



Eventually, the organic and inorganic material produced in the sun-lit surface waters sinks to depth (ballasted by the PIC fraction, e.g. Klaas and Archer 2002) and it is remineralized on its way down the euphotic and twilight zone (Buesseler et al. 2007), entering the deep ocean. Calcium carbonate (CaCO₃) dissolution in the ocean depends mainly on the saturation state (Ω_{cal}), and surface waters are usually supersaturated ($\Omega_{\text{cal}} > 1$) while deeper water is undersaturated with respect to CaCO₃ ($\Omega_{\text{cal}} < 1$) and thus the material is dissolved. The inorganic carbon reach the sediment (mainly CaCO₃) is dissolved in situ, incorporated into the sediments or (when it is organic carbon) used as food for the microbial and faunal communities (Gooday 2002). Pelagic calcification, including that of coccolithophores, contributes to the particle rain from the euphotic zone (Balch et

al. 1996, 2000, 2007; Marsh 2003), with foraminifera and pteropods also contributing a substantial portion of the CaCO_3 exported (Schiebel 2002; Gangsto et al. 2008). Coccolithophore species such as *Gephyrocapsa oceanica* and *Calcidiscus leptoporus* have been found in sediment records and sediment traps in low latitudes and are thought to play an important role in carbon export in those regions (Colmenero-Hidalgo et al. 2004; De Bernardi et al. 2005). It has been suggested from calculations of CaCO_3 coccolith content and sediment trap data that *G. oceanica* and *C. pelagicus* might be the two most influential coccolithophore contributors to global sedimentation fluxes of CaCO_3 (Broerse 2000, Ziveri et al. 2007) although *E. huxleyi* might be an important contributor in higher latitudes (Samtleben and Bickert, 1990; Knappertsbusch and Brummer, 1995; Ziveri et al. 1995, 1996; Broerse et al. 2003).

1.5 Significance and objectives of this study

Recent studies of coccolithophorid sensitivity to increasing atmospheric CO_2 have shown that calcification rates decrease as $p\text{CO}_2$ increases (Riebesell et al. 2000; Zondervan et al. 2001, 2002, Engel et al. 2005, Delille et al. 2005; Langer et al. 2006) with some still debatable exceptions (Iglesias-Rodriguez et al. 2008; Langer et al. 2009; Shi et al. 2009). Studies investigating the combined effect of $p\text{CO}_2$ and temperature have reported growth rates to accelerate as temperature increases and a general decrease in calcification rates for increasing $p\text{CO}_2$ (less pronounced for those at higher temperatures). Studies examining the combined effect of $p\text{CO}_2$ and temperature are limited to *E. huxleyi* at very few levels of $p\text{CO}_2$ (Feng et al. 2008, De Bodt et al. 2010).

In this experiment we used an innovative approach that consisted on extending the number of treatments across a wide range of $p\text{CO}_2$ and two temperatures at the expense of replication per treatment in triplicates. This provides a robust dataset in terms of gradient and the possibility to explore non linear response, for instance following optima. The unique design allows to test lower and upper thresholds of biological production (for different parameters) that may help to

shape biogeochemical modeling formulations in the near future. Model predictions based on *E. huxleyi* experiments provide "biased" data which does not represent realistically the role of coccolithophores in biogeochemical cycles (Ridgwell et al. 2007). It only provides a first order approximation of an ideal situation where the world oceans are only inhabited by *E. huxleyi*. Zondervan et al. (2001) showed that global carbon export production model calculations depend immensely on the input data from e.g. laboratory experiments. For example, there were major changes in the CO₂ feedback to the atmosphere if using a formulation for *E. huxleyi* or *G. oceanica*, or even for *E. huxleyi* grown in a light cycle of 16:8 or 24:0. It is important to incorporate other variables into the experimental design to create conditions similar to those in the "real environment" and generate more realistic predictions of the future ocean. The incorporation of temperature as an extra variable enhances the understanding of the interactive nature of $p\text{CO}_2$ and temperature both in experiments and hopefully in biogeochemical models.

2. MATERIALS AND METHODS

2.1 Experimental Setup

Batch cultures are closed experimental systems where phytoplankton cells are grown in a known volume of culture media, under specific environmental conditions (in this case carbonate chemistry, nutrients, temperature, and light cycle). When phytoplankton cultures grow to high densities they have a strong effect on the carbonate system because of significant DIC drawdown and consumption. A dilute batch culture approach was used in this experiment to avoid major changes in the carbonate system. Artificial seawater (ASW) was prepared according to Kester et al. (1967) because the carbonate chemistry could be easily adjusted. In order to calculate carbonate system parameters the program CO2SYS by E. Lewis and D. Wallace was used (Lewis and Wallace 1997). The dissociation constants used for carbonate system calculations were from Roy et al. (1993) for K1 and K2 for carbonic acid and from Dickson (1990) for K_{SO4} . The pH scale was set to total scale. The program calculated DIC concentrations from given TA and desired pCO_2 , which was used to determine how much had to be added from a 2 mmol/kg Na_2CO_3 stock solution. TA was adjusted through addition of calculated amounts of certified hydrochloric acid (3.571 M HCl) in order to obtain the desired pCO_2 . A stock culture at 400 μatm pCO_2 was initially prepared to acclimate cultures to each corresponding temperature. To ensure acclimation of cultures to each pCO_2 treatment, pre cultures were inoculated from this 400 μatm pCO_2 stock culture into 0.5 L polycarbonate bottles (Nalgene™) and grown for at least 7 generations. These acclimated pre cultures were subsequently used for inoculation of the 2 L experimental bottles (Figure 3). Growth rates obtained from pre culture set-ups with the same conditions as the ones run during the experiments, allowed to estimate growth rates in order not to exceed final cell densities of 30,000 cells ml^{-1} . The main experiments were carried out in 2 L polycarbonate bottles (Nalgene™) with no replicates per treatment at two different temperatures (15 and 20 °C) and a gradient of 12 pCO_2 levels. This innovative approach allows testing a much larger range of pCO_2 by avoiding replicates. The

incubations of pre culture and experimental treatments were carried out in a climate chamber (RUMED Rubarth Apparate GmbH) with an irradiance of $150 \mu\text{mol photon m}^{-2} \text{sec}^{-1}$ and a 16:8 light to dark cycle.

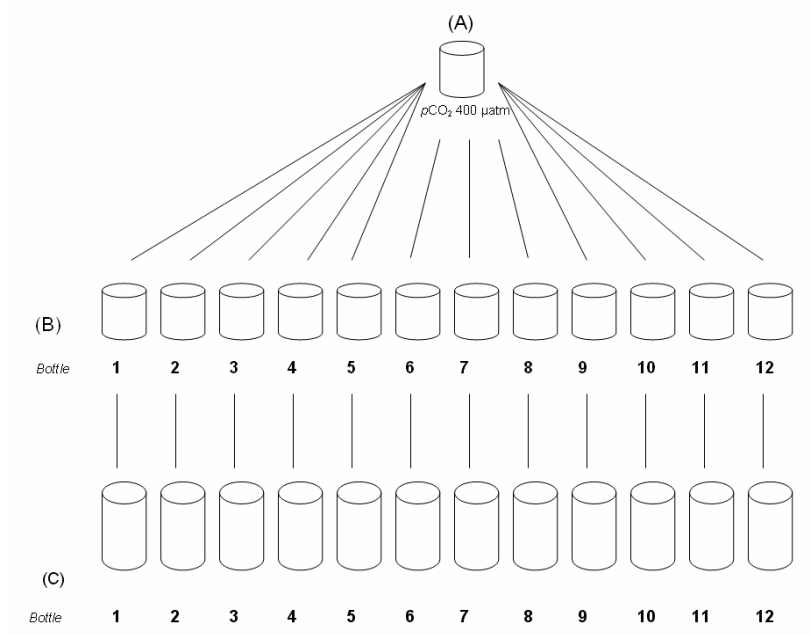


Figure 3. Experimental set-up diagram. (A) stock culture in artificial seawater (ASW) at $\sim 400 \mu\text{atm } p\text{CO}_2$. (B) Pre-cultures at 12 different $p\text{CO}_2$ levels and constant TA of $\sim 2350 \mu\text{mol kg}^{-1}$. (C) Experimental bottles at 12 different $p\text{CO}_2$ levels and constant TA of $\sim 2350 \mu\text{mol kg}^{-1}$.

2.2 *Coccolithophore culture and media*

Gephyrocapsa oceanica (Strain RCC 1303) isolated by Ian Probert in February 1999 from the Atlantic Ocean ($44^\circ 6' \text{ N}$, $1^\circ 5' \text{ W}$, French coast) was used for this experiment. For each experiment, 50 L of ASW were prepared and used for the incubation of pre cultures as well as experimental bottles. Nutrients were adjusted to $64 \mu\text{mol kg}^{-1}$ nitrate [NO_3^-] and $4 \mu\text{mol kg}^{-1}$ phosphate [PO_4^{3-}] to prevent nutrient limitation during the course of the experiment. It has also been shown that addition of Se is required for maximizing growth rates of *G. oceanica* (Danbara et al. 1999) and thus this component was also included (10 nmol kg^{-1}). Vitamins and trace metals were prepared according to Guillard and Ryther (1962) and added according to f/4 and f/8, respectively. Additionally, sterile

filtered NSW (North Atlantic) was added to provide natural trace element components which might have not been supplied by the vitamins and trace metal. The ASW solution (with nutrients, vitamins, natural seawater and trace metals) was then filtered through a 0.2 μm sterile filter directly into the pre culture and experimental bottles. Finally, the carbonate system was set up as described above through addition of Na_2CO_3 and HCl leaving no headspace to avoid equilibration with atmosphere.

2.3 Experimental parameters

Carbonate system parameters, namely DIC and TA were manipulated by addition of Na_2CO_3 and HCl. A range of 12 theoretical $p\text{CO}_2$ treatments (between ~ 40 and $3000 \mu\text{atm}$) were prepared and TA kept constant at $\sim 2350 \mu\text{mol kg}^{-1}$. These conditions “mimic” a scenario of ocean acidification in which $p\text{CO}_2$ increases and TA remains constant (Schulz et al. 2009). The response of *G. oceanica* to these sequential 12 $p\text{CO}_2$ treatments was investigated at 15 and 20 $^{\circ}\text{C}$.

2.4 Sampling and Measurements

Bottles inside the climate chamber were individually rotated daily to ensure homogenous distribution of cells. Sampling always took place two hours after start of the light cycle inside the climate chamber and filtration of the samples was done through a vacuum filtration device (Figure 4). A maximum of three bottles per day was sampled within a period of ~ 2 hours. This was possible by calculating growth rates obtained from pre cultures and different initial cell density inoculations. Since high cell densities take up more DIC and TA and change carbonate chemistry, sampling was carried out before final cell densities reached $30,000 \text{ cells ml}^{-1}$. Sampling started with DIC (to minimize gas exchange with the atmosphere) and continued with particulate matter [particulate organic carbon (POC), total particulate carbon (TPC), and particulate organic phosphorus (POP)] chlorophyll *a*, cell densities and filters for scanning electron microscopy (SEM). Finally, samples were taken for nutrients and TA from the collected filtrate.

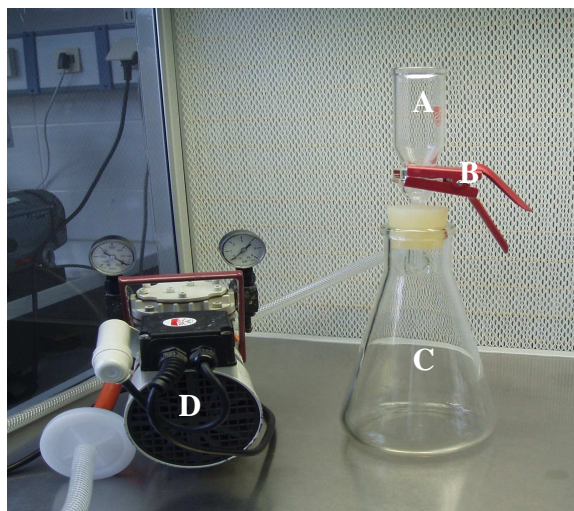


Figure 4. Vacuum filtration device with: (A) filtration funnel (B) filter holder (C) Erlenmeyer Flask for collection of filtrate and (D) vacuum pump.

Dissolved inorganic carbon (DIC)

DIC samples were taken before cell inoculation and at the end of the experiment to monitor the change in DIC throughout the experiment. Samples were gently pressure-filtered through a 0.2 μm sterile filter into 5 ml borosilicate vials and closed airtight. Storage of the samples was in the dark at 4 $^{\circ}\text{C}$ until processing. Samples were processed in a QUAATRO analyzer according to Stoll et al. (2001) with a precision and accuracy of $\sim 20 \mu\text{mol kg}^{-1}$. Calibration of the samples was against certified reference material (Dickson standard Batch # 88, Prof. A.G. Dickson Marine Physical Laboratory, University of California).

Total alkalinity (TA)

TA samples were taken from the collected filtrate ($\sim 400 \text{ ml}$) and stored at 4 $^{\circ}\text{C}$ until processing. TA samples were processed within two weeks and thus not poisoned with HgCl_2 . Samples were measured in duplicates at 20 $^{\circ}\text{C}$ in a Metrohm Basic Titrino 794 titration device with a 0.05 molar HCl according to Dickson et al. (2003). Accuracy and precision of analysis is $\sim 4 \mu\text{mol kg}^{-1}$. Samples were

calibrated against certified reference material (Dickson standard Batch #88, Prof. A.G. Dickson Marine Physical Laboratory, University of California).

Particulate matter [particulate organic carbon-nitrogen (POC, PON), total particulate carbon-nitrogen (TPC, TPN) and particulate organic phosphorous (POP), Chlorophyll *a*]

Samples for particulate matter were taken in duplicates and filtered on GF/F filters (pre-combusted at 500°C for 6 hours) and stored in glass petri dishes (pre-combusted at 500°C for 6 hours). Vacuum pressure during filtration did not exceed 200 mbar. Generally, 400 ml of sample were filtered for POC-PON and 200 ml for TPC-TPN and POP. All samples were stored at -20 °C until analysis.

Total particulate carbon and nitrogen (TPC and TPN)

TPC and TPN (measured simultaneously from one filter) samples were dried overnight at 60 °C and packed into tin boats for analysis. Samples were analyzed with a Euro EA Elemental Analyzer according to Sharp (1974).

Particulate organic carbon and nitrogen (POC and PON)

POC and PON (measured simultaneously from one filter) samples were placed in a desiccator above 37% HCl fuming acid for 2 hours to remove all inorganic carbon and then dried overnight at 60 °C. Analysis followed that of TPC and TPN according to Sharp (1974).

Particulate inorganic carbon (PIC)

Since PIC was not directly measured it was calculated from measured TPC and POC in the following equation:

$$\text{PIC} = \text{TPC} - \text{POC} \quad (\text{equation 6})$$

Particulate organic phosphorous (POP)

POP samples were processed according to Hansen and Koroleff (1999) with the addition of Oxisolv™ as oxidation reagent.

Chlorophyll a (Chl a)

Chlorophyll a was analyzed according to Welschmeyer (1994) and calculated according to the following equation:

$$Chl\ a\ (\mu g\ dm^{-3}) = \frac{F * C * V}{P} \quad \text{(equation 7)}$$

Where F is the fluorescence reading, V the volume of acetone used (ml), P the volume of filtered sample (L) and C the calibration factor (μg Chl a per ml 90 % acetone per instrument fluorescence units, depends on fluorometer)

Cell densities and growth rate (μ)

Samples for quantification of cell densities were taken from each experimental bottle (~10 ml) and after careful mixing. Analysis was done with a Beckman Z2 Coulter® Particle Count and Size Analyzer. In some cases, it was necessary to take samples for microscopic counting because aggregates prevented proper functioning of the cell counts of the Z2 particle counter. Final growth rates were calculated according to the following equation:

$$\mu = \frac{\ln(t_f) - \ln(t_0)}{d} \quad \text{(equation 8)}$$

where t_f represents cell densities at the end of the experiment and t_0 represents initial cell densities, d represents the days between t_0 and t_f .

Nutrients

Nutrient samples (~100 ml) were taken at the beginning of the experiment from the 50 L and at the end of each filtration from the filtrate and stored at 4 °C. Nitrate

(NO₃⁻) and Phosphate (PO₄³⁻) were analysed according to Hansen and Koroleff (1999).

Scanning electron microscopy (SEM)

SEM samples were filtered onto 0.2 µm polycarbonate filters. For each filter, 10 ml of sample were filtered at a pressure < 25 mbar to avoid damaging complete coccospheres, dried at 60 °C for ~1 hour and stored in the dark at room temperature. SEM pictures were used to assess potential morphological effects of different temperatures and *p*CO₂ on *G. oceanica* coccospheres.

2.5 Statistics

Sigmaplot version 10 was used for graphical work. From the program, a nonlinear regression algorithm was used to analyze data and error bars are given as standard error (no triplicate measurements). The statistical P-values for the regression lines were also calculated. A Kolmogorov-Smirnov test was used to assess if data were normally distributed in all cases.

3. RESULTS

3.1 Carbonate System

Measured carbonate system parameters for this study, DIC and TA are given as the average from initial and final concentrations for both experiments (Table 1).

Table 1. Bottle number, calc. $p\text{CO}_2$ (calculated $p\text{CO}_2$ from averages of measured DIC and TA values), DIC_{ave} (average from initial and final DIC concentrations), TA_{ave} (average from initial and final TA concentrations), * (DIC values corrected according to equation 9) at 20 and 15°C. Individual initial and final concentrations of DIC and TA in Appendix AI (20°C) and AII (15°C).

Bottle #	20 °C			15 °C		
	calc. $p\text{CO}_2$ (μatm)	DIC_{ave} ($\mu\text{mol kg}^{-1}$)	TA_{ave} ($\mu\text{mol kg}^{-1}$)	calc. $p\text{CO}_2$ (μatm)	DIC_{ave} ($\mu\text{mol kg}^{-1}$)	TA_{ave} ($\mu\text{mol kg}^{-1}$)
1	50	1571.28*	2339.84	44	1588.45*	2330.57
2	166	1825.68	2295.59	102	1765.76*	2301.63
3	371	1997.90	2287.87	216	1920.26	2275.63
4	488	2053.96	2290.63	290	2012.86	2313.43
5	969	2160.48*	2280.38	476	2083.53	2284.77
6	1052	2161.84*	2268.48	599	2131.16*	2295.31
7	1861	2249.78	2278.15	1133	2216.94*	2286.69
8	1503	2249.11*	2308.59	1165	2230.10*	2296.89
9	2292	2295.07	2296.08	1663	2270.22	2289.52
10	2277	2304.67*	2307.11	1276	2284.90	2342.62
11	2311	2302.53*	2302.68	1421	2321.09*	2365.81
12	2037	2295.58	2313.72	2774	2332.56*	2281.04

In some cases, measured final DIC concentrations were higher than initial DIC concentrations, or initial measured DIC concentrations were too high compared to calculated concentrations (indicated with * in Table 1). In these specific cases, data were corrected by calculating final (or initial) DIC concentrations from TPC buildup according to (Appendix AI):

$$\text{DIC}_i - \text{DIC}_f = \text{TPC-buildup} \quad (\text{equation 9})$$

A clear gradient of 12 $p\text{CO}_2$ levels ranging from 44-2774 μatm at 15°C and 50-2311 μatm at 20°C was established. Appendix AI and BI include the measured DIC samples without the correction as well as the carbonate system parameters $p\text{CO}_2$, CO_3^{2-} , HCO_3^- , CO_2 , $\Omega\text{-Ca}$ and pH_{total} .

3.2 Growth Rates

Growth rates at 15 and 20 °C followed an optimum curve behavior with optimum growth at ~216-476 and ~ 488-1052 $\mu\text{atm } p\text{CO}_2$, respectively. Lowest growth rates were found below ~44 μatm and above ~2774 $\mu\text{atm } p\text{CO}_2$, with 0.13 d^{-1} at 15°C. Lowest growth rates at 20°C were found below ~50 μatm and above ~2037 $\mu\text{atm } p\text{CO}_2$ with 0.29 and 0.36 d^{-1} . Data for both temperatures was fitted to the non-linear regression equation #10, where the first part of the equation $[ax/(b+x)]$ represents a Michaelis Menten kinetic and the second part $[-cx]$ a linear negative effect of increasing atmospheric CO_2 (most likely due to changing pH):

$$f = ax / (b + x) - cx$$

(equation 10)

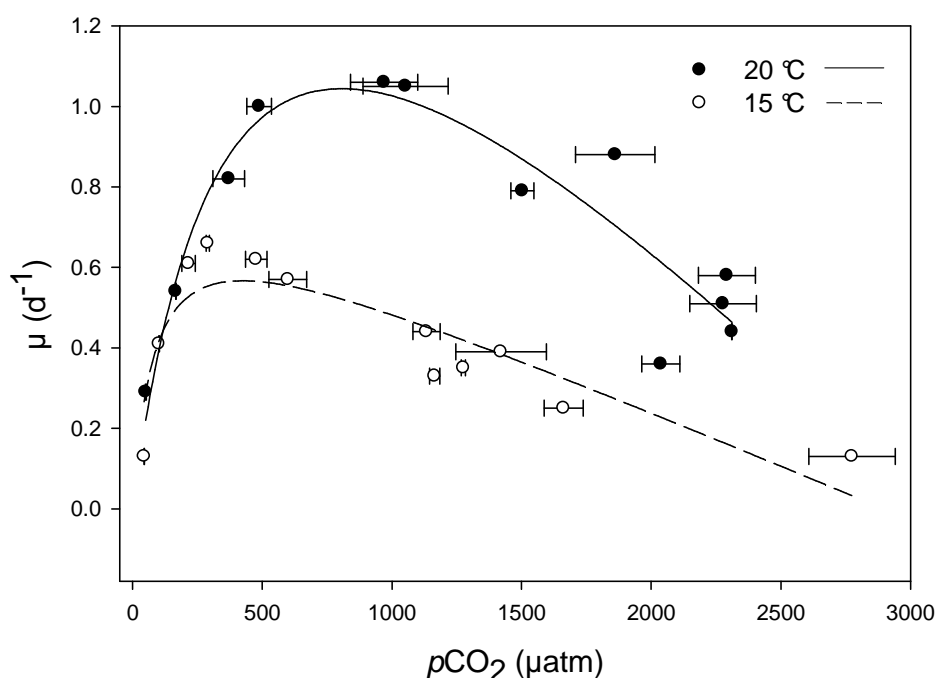


Figure 5. Growth rates $\mu \text{ (d}^{-1}\text{)}$ at 15 and 20 °C against calculated $p\text{CO}_2$. Error bars indicate standard error (SE)(from initial and final $p\text{CO}_2$). At 15 °C: $f = 0.82x / (86.65 + x) - 0.0003x$ ($r^2 = 0.89$, $P < 0.01$). At 20°C: $f = 2.50x / (442.5 + x) - 0.0007x$ ($r^2 = 0.92$, $P < 0.01$).

3.3 Cell quotas

Chlorophyll a cell quotas

The Chl. a content per cell at 15 and 20 °C was rather constant with a slightly decreasing trend (Figure 6a). Highest Chl. a cell quotas at 15°C were found at ~290-599 $\mu\text{atm } p\text{CO}_2$ and at 20°C at ~371-1800 $\mu\text{atm } p\text{CO}_2$. We observed an almost doubling of Chl. a cell quotas at 20 °C compared to 15 °C in the ~290-1800 μatm range.

POC cell quotas

POC cell quotas in both experiments showed a slightly increasing trend towards increasing $p\text{CO}_2$ (Figure 6b). POC per cell at 15 °C showed highest cell quotas at $p\text{CO}_2$ levels of ~1663-2774 μatm . At 20°C, data points were a bit more noisy with highest values at $p\text{CO}_2$ levels ~1506-2040 μatm and slightly lower values at $p\text{CO}_2$ levels of ~2282-2355 μatm . Lowest cell quotas at 15 °C were observed in the lowest $p\text{CO}_2$ treatments with the exception of one possible outlier at ~1742 $\mu\text{atm } p\text{CO}_2$ with 11.31 pg C cell⁻¹. A possible outlier at 20°C might be the first $p\text{CO}_2$ level in which POC content is higher (19.24 pg C cell⁻¹ at ~50 $\mu\text{atm } p\text{CO}_2$).

PIC cell quotas

PIC cell quotas at 15 and 20 °C showed a decrease towards increasing $p\text{CO}_2$ (Figure 6c). Highest cell quotas at 15°C were found at levels of ~44-102 μatm and at 20°C at ~166-488 $\mu\text{atm } p\text{CO}_2$. One outlier at 15°C might be found at ~1549 $\mu\text{atm } p\text{CO}_2$ with 12.68 pg C cell⁻¹ as the lowest measured value. At 20°C data points were a bit more scattered than at 15°C and no clear trends are observed.

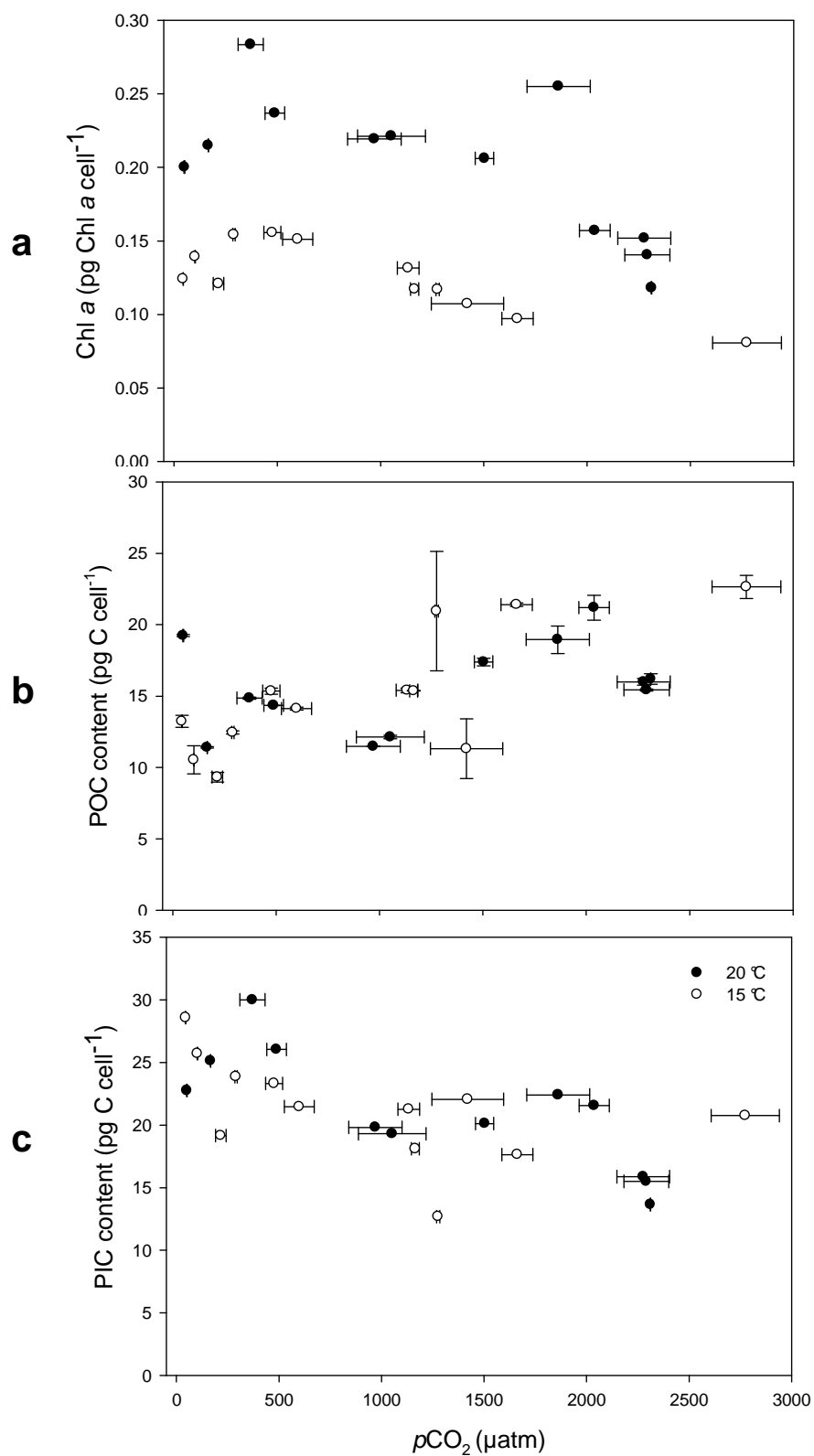


Figure 6. Cell quotas plotted against calculated $p\text{CO}_2$ with a) Chl. a, b) POC and c) PIC. Error bars indicating standard error (SE).

3.4 Production rates

Chlorophyll a production rates

Chl. a production at 15 and 20 °C followed an optimum curve behavior (Figure 7a). Chl a production at 15 °C peaked at ~290-599 $\mu\text{atm } p\text{CO}_2$ and at ~371-1052 $\mu\text{atm } p\text{CO}_2$ at 20°C. Production rates at 20°C were almost doubled than at 15 °C in the 300-900 $\mu\text{atm } p\text{CO}_2$ range. Lowest production rates at both temperatures were observed below ~150 μatm and above ~1663 μatm .

POC production rates

POC production at 15 and 20 °C followed an optimum curve behavior (Figure 7b). POC production at 15 °C peaked at ~299-599 $\mu\text{atm } p\text{CO}_2$ and at ~371-969 $\mu\text{atm } p\text{CO}_2$ at 20°C. Lowest POC production rates were observed at lowest and highest $p\text{CO}_2$ levels for both experiments, below ~100 μatm and above 2000 μatm .

PIC production rates

Calcification or "PIC production" in both experiments followed an optimum curve behavior and faster calcification at 20 °C (Figure 7c). Calcification rates at 20 °C were almost twice as fast as in 15 °C for similar $p\text{CO}_2$ levels. Calcification at 15°C showed an optimum at ~290-476 $\mu\text{atm } p\text{CO}_2$ and ~371-488 μatm at 20°C. Lowest calcification rates were observed below ~50 μatm and above 2500 $\mu\text{atm } p\text{CO}_2$.

Table 2. Statistical data summary for production rates at 15 and 20 °C. Data were fitted to the general equation #11. Shown are values for r^2 , P value, and equation #11 coefficients. Data normally distributed according to Kolmogorov-Smirnov test (Figure 3a-c).

20 °C				15 °C		
	Chl a production	POC production	Calcification	Chl a production	POC production	Calcification
r^2	0.82	0.60	0.86	0.75	0.76	0.69
P	< 0.01	< 0.01	< 0.01	< 0.01	< 0.01	< 0.01
K-S test	0.20	0.15	0.20	0.2	0.11	0.15
coefficient a	0.67	29.79	48.26	0.12	12.08	16.97
b	482.26	382.27	268.31	92.39	145.18	64.56
c	0.0002	0.0074	0.0155	0.000045	0.0034	0.006

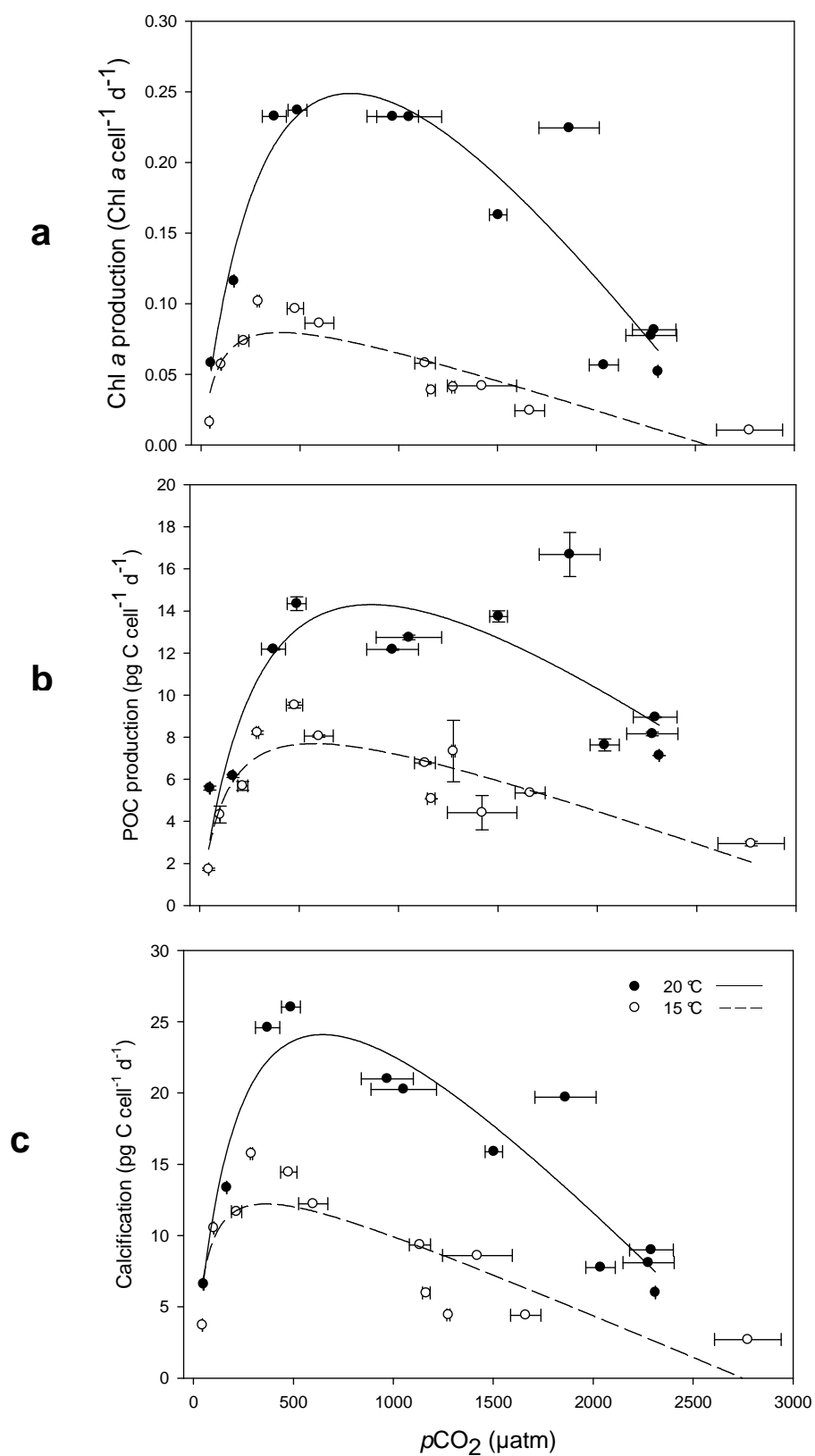


Figure 7. Production rates plotted against calculated $p\text{CO}_2$ for a) Chl. a, b) POC and c) calcification (PIC production). Error bars indicating standard error (SE). Statistical summary in Table 2.

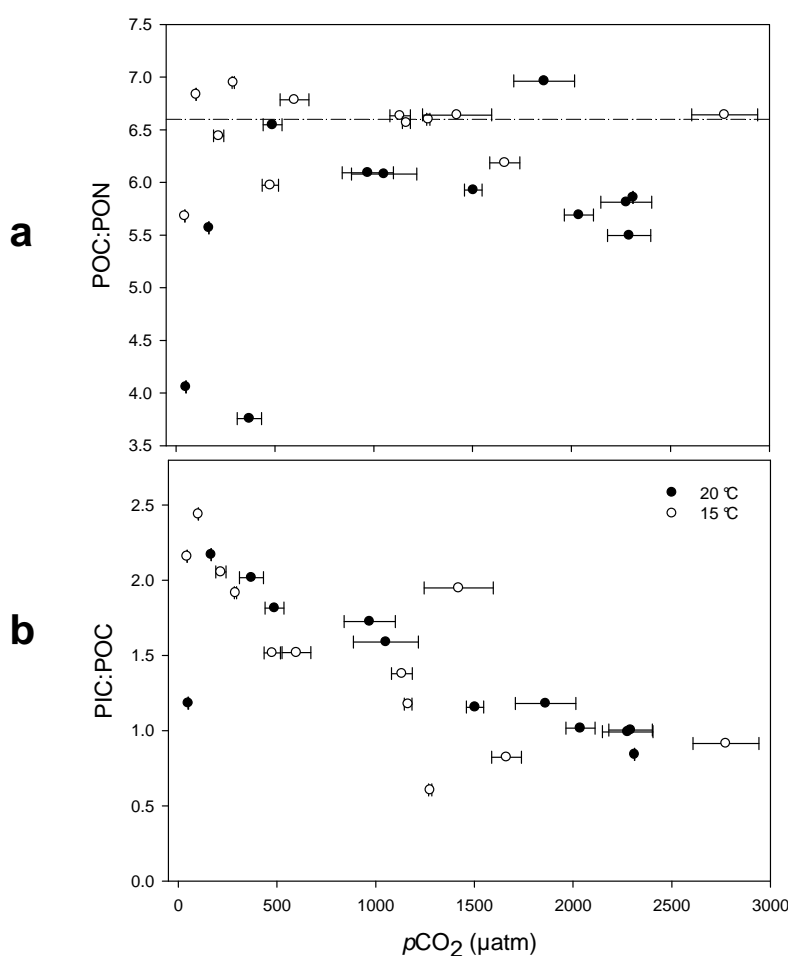
3.5 Ratios

POC:PON ratios

POC:PON ratios were similar to the expected Redfield ratio for C:N of 106:16 (Redfield 1958). Ratios for the lowest $p\text{CO}_2$ levels at 20 °C were observed to be slightly lower with ~4 (Figure 8a). POC:PON ratios at 15°C are slightly higher than those at 20°C.

PIC:POC ratios

PIC:POC ratios linearly decreased towards increasing $p\text{CO}_2$ (Figure 8b). At 15 °C a clear linear decrease started at ~44 μatm with the exception of one possible outlier at ~1549 μatm with 0.61. At 20 °C, the linear decrease started at ~166 μatm $p\text{CO}_2$ (with a possible outlier at lowest $p\text{CO}_2$ value of ~50 μatm $p\text{CO}_2$ and PIC:POC ratio of close to ~1). No effect of temperature was observed.



Figures 8. Ratios plotted against $p\text{CO}_2$ with a) POC:PON and b) PIC:POC. Error bars indicate standard error (SE). Dashed line in a) indicates Redfield ratio of C:N (106:16).

3.6 SEM images

SEM images are shown in Figures 9A-F and 10A-F from six out of 12 $p\text{CO}_2$ levels at 15 and 20°C. Clear signs of cell malformation were first observed at $\sim 1417 \mu\text{atm}$ at 15°C and at $\sim 1505 \mu\text{atm}$ at 20°C.

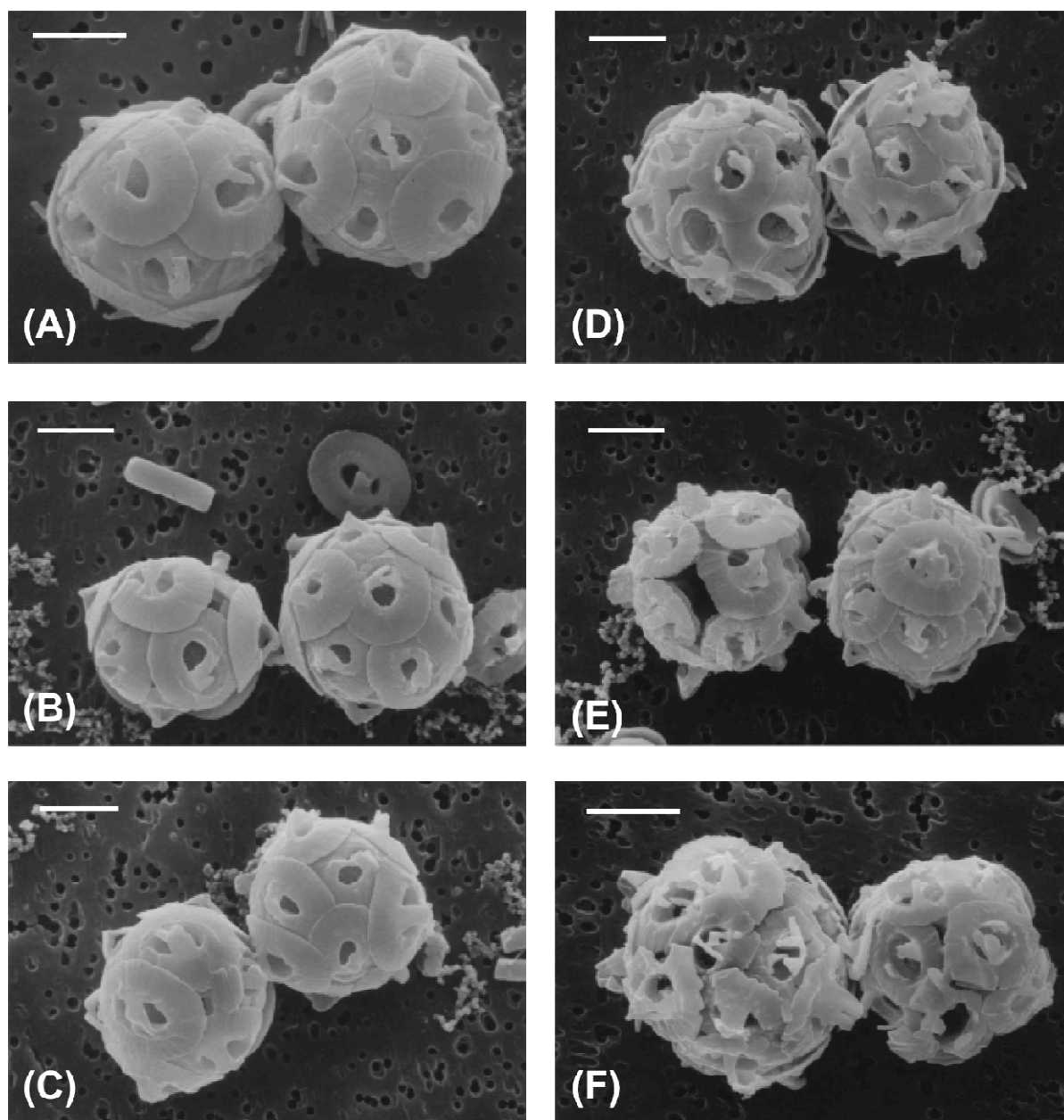


Figure 9. SEM pictures at 15 °C for A) ~ 44 , B) ~ 216 , C) ~ 476 , D) ~ 599 , E) ~ 1663 and F) $\sim 2774 \mu\text{atm}$ $p\text{CO}_2$. Scale bar indicates 3 μm .

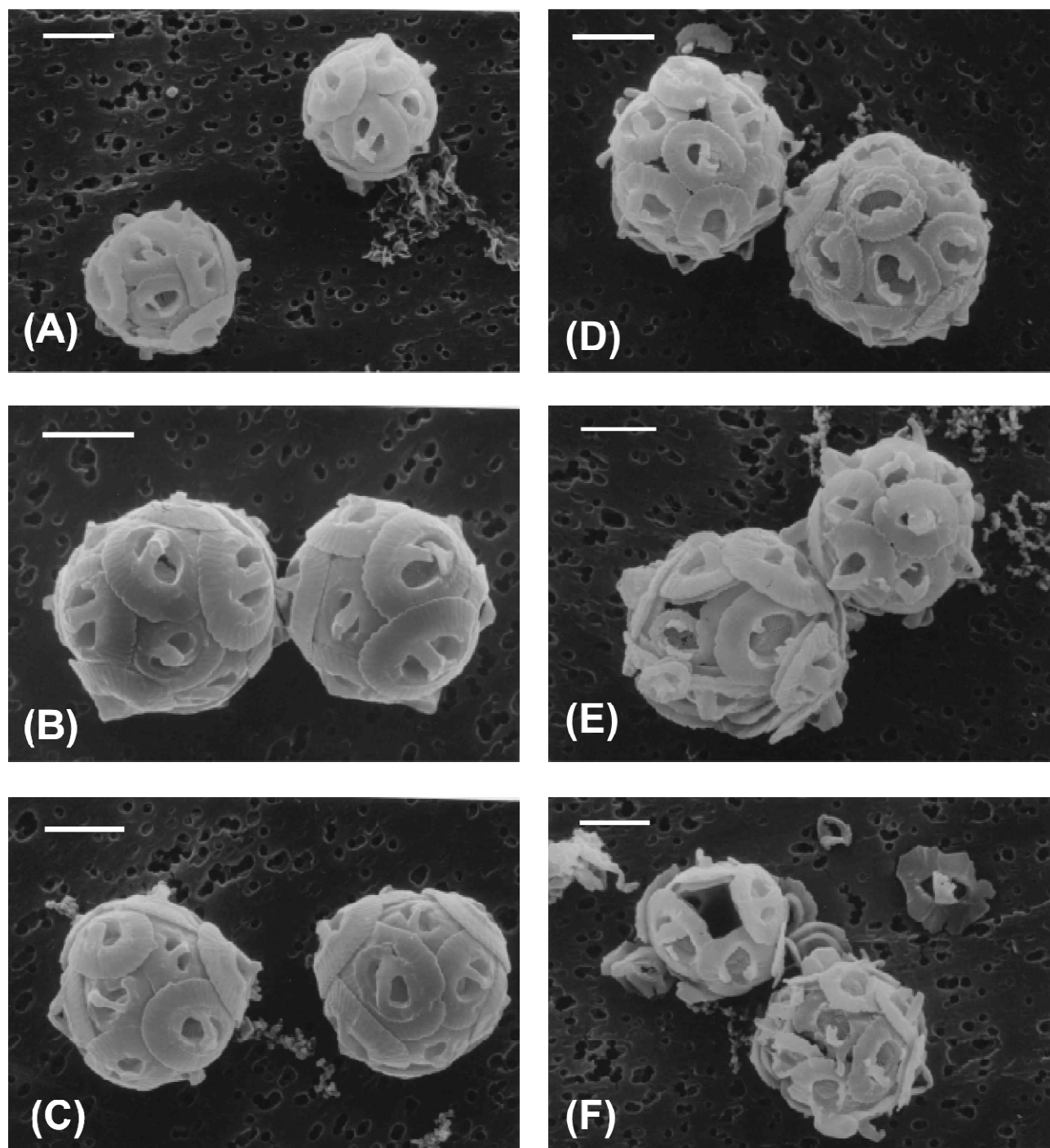


Figure 10. SEM pictures at 20 °C for A) ~50, B) ~371, C) ~969 , D)~1503, E) ~2292, F) ~2037 $\mu\text{atm } p\text{CO}_2$. Scale bar indicates 3 μm .

4. DISCUSSION

4.1 Growth rates

Literature for growth rates at different temperatures of *G. oceanica* is limited (Rhodes et al. 1995, Conte et al. 1998, Riebesell et al. 2000, Zondervan et al. 2001, Buitenhuis et al. 2008, Rickaby et al. 2010) but reported growth rates from other studies at temperatures between 12 and 30 °C, are similar to those obtained in the present study (Figure 12). The increasing trend in growth rate for increasing temperature was observed in all studies which investigated more than 1 temperature and especially clear in Conte et al. (1995) who used 6 temperatures. Nevertheless, rates from Conte et al. (1995) and Rhodes et al. (1995) were slightly higher than those from other studies at the same temperature (Zondervan et al. 2001; Buitenhuis et al. 2008; Rickaby et al. 2010 and the present study).

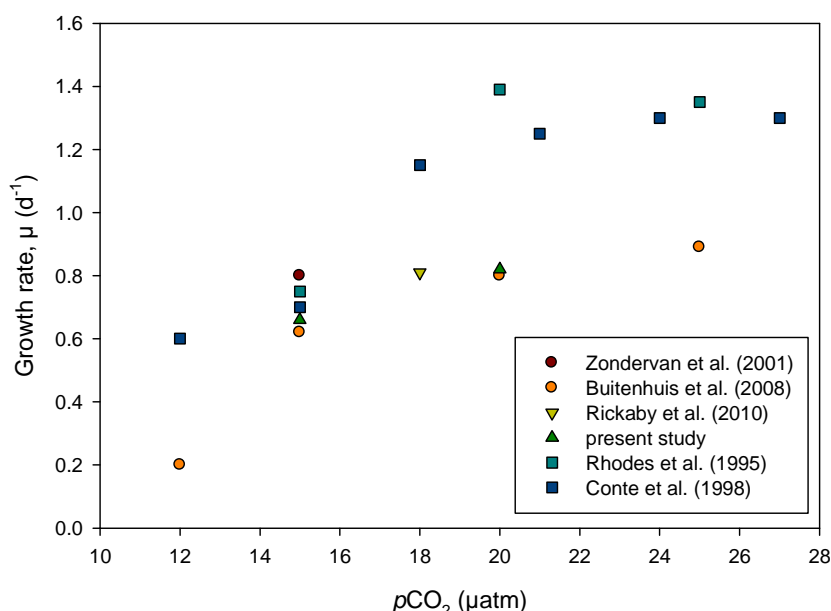


Figure 12. Growth rate of *G. oceanica* as a function of temperature for five published studies and the one presented here.

In a study with six different coccolithophore species at six different temperatures, Buitenhuis et al. (2008) reported that *G. oceanica* was the only species to still increase its growth rate at temperatures of up to 25°C, which was argued to be consistent with the biogeographical distribution of *G. oceanica* constrained to tropical and temperate waters with temperatures ranging between 13 and 26°C (McIntyre and Be 1967). Temperature plays an important role because metabolic activity accelerates with increasing temperature within a certain level (Lund 1949, Talling 1955, Eppley 1979). For this study, a 20% increase in growth rate was observed

from 15°C to 20°C at $p\text{CO}_2$ levels of ~476-1500 μatm . Similar results with a 22% increase were found by Buitenhuis et al. (2008), while a 44% increase for Conte et al. (1998) and 46% by Rhodes et al. (1995) from 15 to 20°C at near-ambient $p\text{CO}_2$ levels (~250-600 μatm).

In addition to temperature, $p\text{CO}_2$ is another parameter affecting the response of growth rates in *G. oceanica*. Two previous studies have investigated changes in growth rate in *G. oceanica* in response to increasing $p\text{CO}_2$ (Zondervan et al. 2001 and Rickaby et al. 2010) and the results are in general consistent to those obtained in the present study (Figure 13).

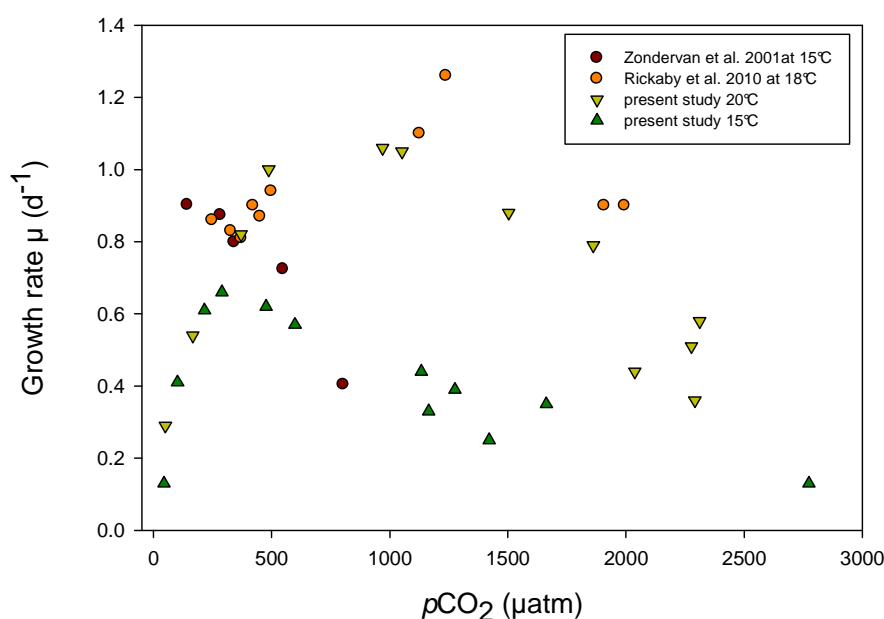


Figure 13. Growth rate of *G. oceanica* as a function of $p\text{CO}_2$ in different studies at temperatures of 15-20°C.

For the present study, lowest growth rates at 20 and 15°C were observed at ~44-160 μatm $p\text{CO}_2$ levels. Optimum growth rates were observed at ~216-476 μatm $p\text{CO}_2$ levels at 15°C and at ~488-1052 μatm $p\text{CO}_2$ at 20°C, a clear shift to higher $p\text{CO}_2$ optimum at increasing temperature. Growth rates from Zondervan et al. (2001) are slightly higher than those from this experiment at the same temperature and this could be attributed to a strain-specific responses (Table 3 and 4). Growth rates from Rickaby et al. (2010) at 18°C showed optima shifted to higher $p\text{CO}_2$ levels (~1126-1237 μatm $p\text{CO}_2$), similar to our results at 20°C.

Table 3. Culture conditions for studies on *G. oceanica* growth rates. “Unknown” $p\text{CO}_2$ referring to no carbonate system manipulation in the experiment.

	Rhodes et al. 1995	Conte et al. 1998	Zondervan et al. 2001	Buitenhuis et al. 2008	Rickaby et al. 2010	present study
$p\text{CO}_2$ (μatm)	unknown	unknown	~341	unknown	~371	~381
light intensity ($\mu\text{mol m}^{-2}\text{s}^{-1}$)	100	100	150	180	200	150
light cycle (light:dark)	14:10	16:8	16:8	14:10	16:8	16:8
Temperature	15, 20, 25	12, 15, 18, 21, 24, 27	15	12, 15, 20, 25	18	15, 20

4.2 POC production rates

An optimum curve in POC production rates at both temperatures was observed for increasing $p\text{CO}_2$ levels, production rates at 20°C slightly higher than at 15°C (Figure 7b). Results are generally consistent with published data (Riebesell et al. 2000, Zondervan et al. 2001 and Rickaby et al. 2010) on *G. oceanica*. Although, for Zondervan et al. (2001) and Rickaby et al. (2010) reported POC production rates, 2 and 3 times higher for present $p\text{CO}_2$ levels at 15 and 18°C, respectively (Figure 13).

Possible reasons for the significant differences could be attributed to cellular POC quotas, related to cell size and strain-specific responses (Table 4). POC cell quotas for Zondervan et al. (2001) ranged from 28-80 pg C cell⁻¹ and 31-56 pg C cell⁻¹ for Rickaby et al. (2010) while in the present study POC quotas ranged from 9-23 pg C cell⁻¹ at both temperatures.

The strain used by Rickaby et al. (2010) was bigger (~4.5-5.5 μm in diameter, ~65 μm^3) than the one used in this experiments (~3-4.5 μm in diameter, 28 μm^3) and thus POC cellular quotas could be argued higher if only considering size.

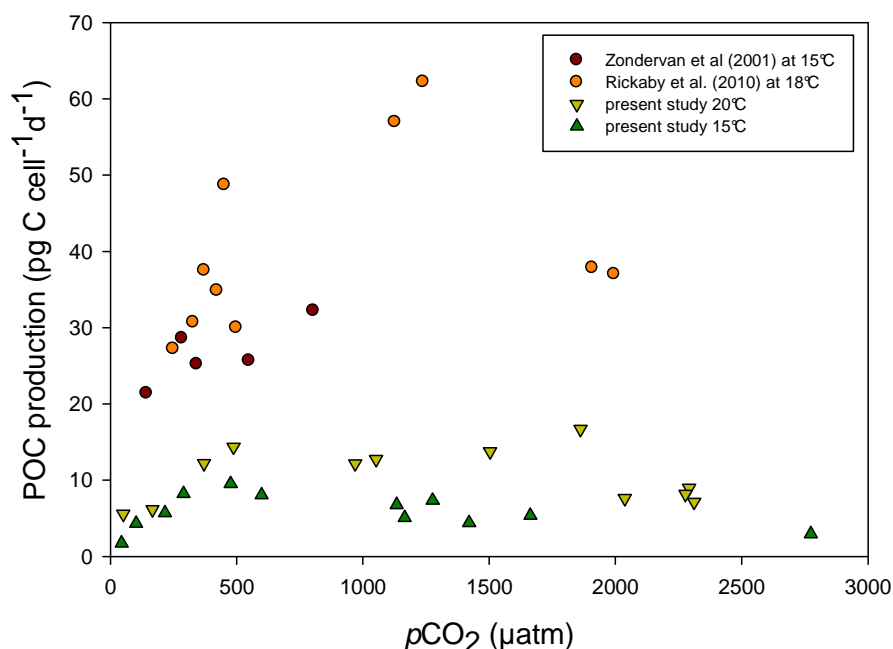


Figure 14. POC production as a function of $p\text{CO}_2$ for this study and published data. Zondervan et al (2001) at 15°C and Rickaby et al (2010) at 18°C.

Comparing mean cell volume of $\sim 65 \mu\text{m}^3$ from Rickaby et al. (2010) with that in the present study of $28 \mu\text{m}^3$ is likely that their cellular contents are twice or three times higher than the ones in this experiment. On the other hand, for POC cellular contents increasing $p\text{CO}_2$ seemed to be a defining factor. POC cellular quotas increased for increasing $p\text{CO}_2$ while no clear effect of temperature on cellular POC content was observed between experiments.

4.3 Calcification rates

Calcification rates were similar to those reported by Zondervan et al. (2001) but considerably lower compared to those from Rickaby et al. (2010) (Figure 16). Some of these differences could be attributed to different culture conditions shown in Table 3 and 4. While this study and Zondervan et al. (2001) used a strain isolated from the North Atlantic (French coast and Portuguese coast, respectively). Rickaby et al. 2010 used a strain isolated from the Pacific Ocean (Gulf of California). The Gulf of California is known for its nutrient rich waters with temperatures ranging from 9-27°C, while the North Atlantic temperature varies from 4-17°C on an annual basis. Calcification being a light dependant, energy requiring process (Feng et al. 2008) might help understand the higher calcification rates from Rickaby et al. (2010)

compared to those observed in this experiment incubated at slightly lower light intensities.

Table 4. Comparison of incubation conditions for studies investigating the effect of increasing $p\text{CO}_2$ on *G.oceanica*, with temperature, light intensity, the origin of where specific strain was isolated and how each study manipulated the carbonate system.

	Zondervan et al. 2001	Rickaby et al. 2010	present study
Temperature (°C)	15	18	15 and 20
light intensity ($\mu\text{mol m}^{-2}\text{s}^{-1}$)	150	200	150
nutrient concentrations ($\mu\text{mol/kg NO}_3^-$ and PO_4^{3-})	100 and 6.25	100 and 6.25	64 and 4
origin of strain	North Atlantic, Portuguese coast	Pacific ocean, Gulf of California	North Atlantic, French coast
carbonate manipulation	addition of HCl and NaOH	HCl and CO_2 bubbled	Na_2CO_3 and HCl

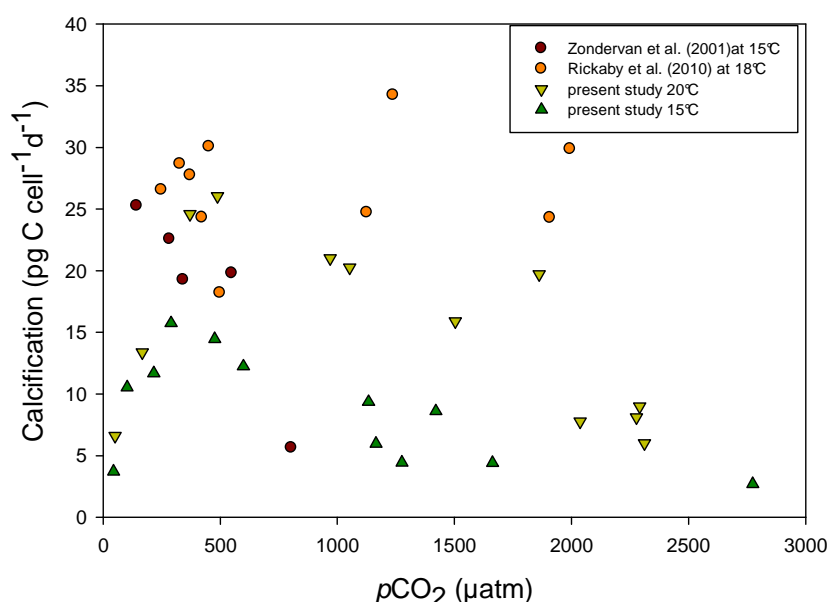


Figure 15. Calcification rates against $p\text{CO}_2$. Comparison from studies by Zondervan et al. 2001 (at 15°C), Rickaby et al. 2010 (at 18°C) and the study presented here (at 15 and 20°C).

The present study showed that calcification rates at both temperatures followed an optimum curve with maximum calcification rates at ~ 290 - $488 \mu\text{atm } p\text{CO}_2$ and a 60% increase in calcification rates from 15 to 20°C at optimum (Figure 7c). An optimum curve trend is not apparent for data by Zondervan et al. (2001) probably since their range in $p\text{CO}_2$ was lower (~ 143 - $803 \mu\text{atm}$) than for our experiments (~ 44 - $2774 \mu\text{atm}$). A different response to increasing $p\text{CO}_2$ was observed for the Pacific strain of Rickaby et al. (2010) with reported calcification rates at 18°C remaining rather unaffected by increasing $p\text{CO}_2$ (18.20 - $34.24 \text{ pg C cell}^{-1} \text{ d}^{-1}$) in a range of ~ 250 - $2000 \mu\text{atm } p\text{CO}_2$ (taking into consideration their data is much more

scattered and the detection of optimum is rather difficult). At 15°C an ~83% reduction in calcification rates from ~290 $\mu\text{tm } p\text{CO}_2$ to ~2774 $\mu\text{atm } p\text{CO}_2$ was observed while a ~75% decrease in calcification rates was observed at 20°C from present to highest $p\text{CO}_2$ levels (~381 and 2356 μatm , respectively). The apparent decrease in calcification rates following the optimum is caused by the decrease in cellular PIC quotas and growth rates observed at both temperatures as $p\text{CO}_2$ increases. Data for values at lower and highest end of $p\text{CO}_2$ levels (as for the present study) might be helpful to clarify trends and optimum production rates for different species and strains. Although calcification rates may still vary due to strain-specific responses, calcification in relation to increasing $p\text{CO}_2$ is temperature independent. Cellular PIC content at 15 and 20°C in this study decreased slightly for increasing $p\text{CO}_2$ and remained unaffected by temperature (Figure 7c). Slightly higher cellular PIC quotas were reported by Zondervan et al. (2001) and Rickaby et al. (2010). As for cellular POC contents, coccolith size might be responsible for this difference but not as pronounced as in POC because of volume ($4\pi r^3/3$) to surface area ($4\pi r^2$). Cellular POC quotas for Rickaby et al. (2010) were estimated to be ~65 μm^3 and ~28 μm^3 for the present study. Meanwhile cellular PIC quotas were estimated as surface area which for Rickaby et al. (2010) would be ~78 μm^2 and ~44 μm^2 .

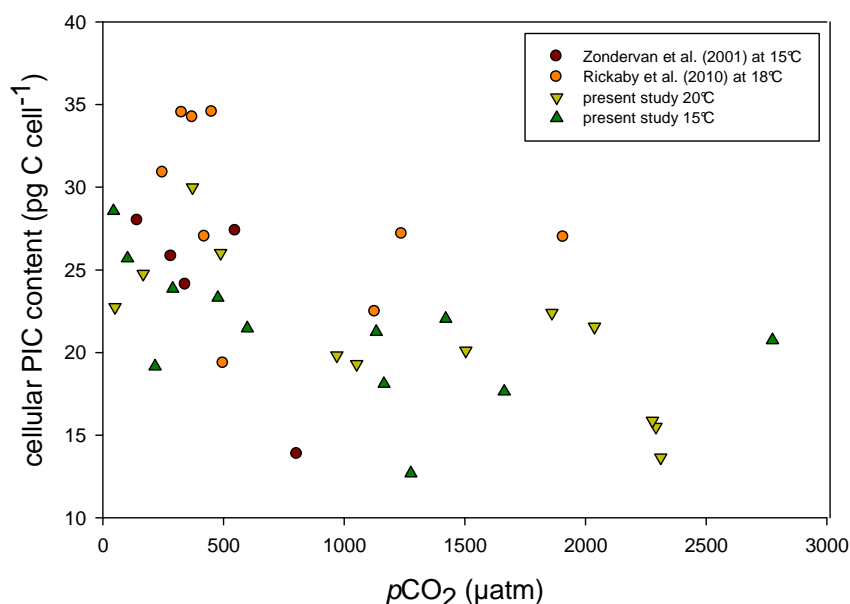


Figure 15. Cellular PIC content as a function of $p\text{CO}_2$ for this study and published data by Zondervan et al. (2001) and Rickaby et al. (2010) at 15 and 18°C, respectively

4.4 Element ratios

PIC:POC ratios have been reported to decrease with increasing $p\text{CO}_2$ in *G.oceanica* (Riebesell et al. 2000, Zondervan et al. 2001, Rickaby et al. 2010) as well as for *E. huxleyi* (Riebesell et al. 2000; Zondervan et al. 2001; Feng et al. 2008; Langer et al. 2009; De Bodt et al. 2010). In the present study, cellular PIC content was higher than cellular POC content, which lead to higher PIC:POC ratios compared to those from Zondervan et al. (2001) and Rickaby et al. (2010).

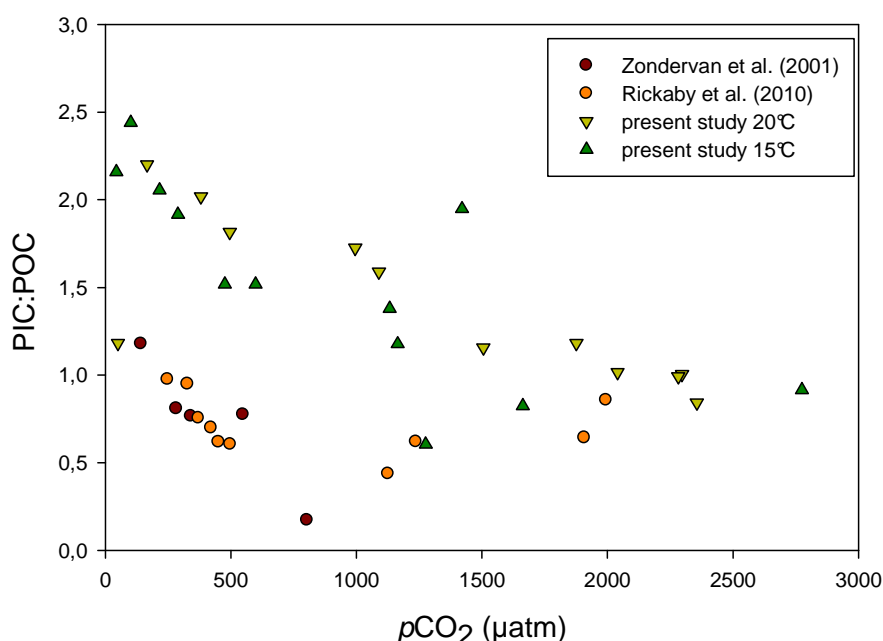


Figure 17. PIC:POC ratios as a function of $p\text{CO}_2$ from studies by Zondervan et al. (2001) at 15°C, Rickaby et al. (2010) at 18°C and the present study at 15 and 20°C.

Lower values in Zondervan et al. (2001) and Rickaby et al. (2010) are generally caused by high POC content in their studies. Meanwhile, data by Rickaby et al. (2010) showed cellular POC and PIC contents to be scatterly, making it difficult to interpret their PIC:POC data. For the experiments presented in this study, PIC:POC at both temperatures decreased at increasing $p\text{CO}_2$ and had similar values for similar $p\text{CO}_2$ levels. A 68% decrease from ~ 290 µatm $p\text{CO}_2$ to highest $p\text{CO}_2$ was observed at 15°C while a 58% decrease in PIC:POC for similar $p\text{CO}_2$ values was observed at 20°C. No effect of temperature was observed in PIC:POC for the present study.

4.5 Comparison to other coccolithophores

Presently *E. huxleyi* dominates all studies carried out to date both in terms of experiments and modeling (Ridgwell et al. 2009, Nisumma et al. 2010). Thus, it is worthwhile to compare sensitivities known for *Emiliana huxleyi* with that of other coccolithophores. The growth rate response of *E. huxleyi* to increasing temperature was the same as for *G. oceanica*, with increasing values at higher temperatures (Feng et al. 2008). Brand et al. (1982) found a 20% increase in growth rates from 16 to 26°C in *E. huxleyi* from the Gulf of Main and a 60% increase from the Sargasso Sea clones. This contradicts results from Buitenhuis et al. (2008) which reported growth rates of *E. huxleyi* to decrease at temperatures higher than 20°. The response of *E. huxleyi* to increasing $p\text{CO}_2$ regarding POC production and calcification rates was similar to those obtained in this study, considering *G. oceanica* to be more sensitive (Zondervan et al 2001). Zondervan et al. (2001) reported that *E. huxleyi* increased its POC production rates by 8.5% (from pre-industrial to expected year 2100 $p\text{CO}_2$ estimates) while for the present study POC production rates increased 17% at 15°C and 14% at 20° (from ~290-1000 $\mu\text{atm } p\text{CO}_2$). De Bodt et al. (2010) and Feng et al (2008) also found increasing POC production rates for increasing $p\text{CO}_2$. Calcification rates in the present study decreased by 41% at 15°C and 18% at 20°C (from ~290-1000 $\mu\text{atm } p\text{CO}_2$) while Zondervan et al.(2001) reported a decrease in calcification for *E. huxleyi* of about 16% (from pre-industrial to year 2100 $p\text{CO}_2$ estimates). A PIC:POC linear decrease was found in all studies (Zondervan et al. 2001, Feng et al. 2008, De Bodt et al. 2010 and the present study) for increasing $p\text{CO}_2$ with no apparent effects of temperature.

Langer et al. (2006) studied the response of *Calcidiscus leptoporus* and *Coccolithus pelagicus* to changing carbonate chemistry and found an optimum curve response in *C. leptoporus* for POC production and calcification rates while *C. pelagicus* showed a constant POC and PIC production to increasing $p\text{CO}_2$ (in a range of ~150-900 $\mu\text{atm } p\text{CO}_2$). PIC:POC ratios from Langer et al. (2006) showed an optimum curve behavior for *C. leptoporus* and a constant PIC:POC ratio for *C. pelagicus*.

Bach (2009) investigated the response of *E. huxleyi* to changing $p\text{CO}_2$ and constant pH (to separate pH and $p\text{CO}_2$ effects) and concluded that at lower $p\text{CO}_2$ levels (left from optima) the defining factor for growth rates and POC production was $p\text{CO}_2$ since at lower $p\text{CO}_2$ levels there is carbon limitation. Meanwhile, at higher $p\text{CO}_2$ levels (right from optima), pH was the defining factor. In this study, lower growth rates, POC

production and calcification rates were found at both lower and higher $p\text{CO}_2$ levels for both temperatures and SEM images revealed that at lower $p\text{CO}_2$ coccoliths were completely formed, while at higher levels there were clear signs of malformations.

Comparing the optima for growth and POC production rates in *E. huxleyi* reported in Bach (2009) and those of the present study confirms that *G. oceanica* is more sensitive (as mentioned in Zondervan et al. 2001) to changes in pH. Moreover, it is likely that CO_2 limitation at low $p\text{CO}_2$ and negative effects of pH at high $p\text{CO}_2$ are a common feature in coccolithophores. The dependence of their sensitivities to both parameters then shapes the form of the respective optimum response curve. Studies that did not find optima (Zondervan et al. 2001, Langer et al. 2006) usually had a more narrow $p\text{CO}_2$ range, most likely preventing their detection. For this study, optima for growth, POC production and calcification rates were slightly shifted towards higher $p\text{CO}_2$ levels at 20°C, probably connected to an increased carbon demand at overall higher rates.

In essence, it seems that all coccolithophores studied so far in the context of ocean acidification have, although individual responses to increasing carbon dioxide at decreasing pH, still similar cellular regulatory mechanisms for calcification and photosynthesis.

4.6 Summary and future perspectives

Experiments at two temperatures provided information on the combined effects of temperature and $p\text{CO}_2$ on growth rates, POC production and calcification rates of *G. oceanica*. Higher calcification and POC production rates on *G. oceanica* for increasing temperature were observed while sensitivity to changing carbonate chemistry seemed to be similar (decreasing as $p\text{CO}_2$ increases) although shifted optimum to higher $p\text{CO}_2$ levels at higher temperatures. This almost-doubling in production rates can be directly attributed to growth rates since temperature had no effect on cellular POC and PIC cellular contents. Even if temperature played an effect by increasing productivity rates, the changes in PIC:POC were temperature independent. Ideally the results obtained from these experiments will further contribute to future modeling predictions of biogeochemical cycles in response to changing environmental conditions.

AI. Carbonate system

The reason for using ASW as experimental media was to ensure carbonate system parameters important for this study (DIC and TA) to be controlled and manipulated as desired. Problems with obtaining the target $p\text{CO}_2$ could be attributed to storing and/or measuring of DIC samples as well as slight higher/lower measured target TA ($2350 \mu\text{mol kg}^{-1}$) or a combination of both. This was problematic with the lowest range of target $p\text{CO}_2$ treatments. Measured DIC samples in the lower $p\text{CO}_2$ range showed measured concentrations to be $\pm 100\text{-}200 \mu\text{mol kg}^{-1}$ higher than expected from DIC additions; this could be attributed to CO_2 ingassing (either from storage, during sampling or measuring). For this matter, individual DIC_i , DIC_f , TA_i and TA_f measurements for each treatment had to be closely analyzed to make sure they correlated with each other. For cases in which DIC_f was higher than DIC_i (common case) then DIC_f was calculated from TPC buildup (marked in red in AI and AIII). Although individual target $p\text{CO}_2$ values were not achieved in its entirety, the wide range in calculated $p\text{CO}_2$ values allowed for an extensive test range in $p\text{CO}_2$. In future experiments it would be recommended that samples are processed within days of sampling and/or new storing techniques developed.

**All
20°C**

Bottle #	calculated $p\text{CO}_2$ (μatm)	μ (cell d^{-1})	Cell densities		uncorrected DIC ($\mu\text{mol kg}^{-1}$)		corrected DIC ($\mu\text{mol kg}^{-1}$)		TA ($\mu\text{mol kg}^{-1}$)	
			initial	final	initial	final	initial	final	initial	final
1	50	0.29	513	3168	1588.76	1925.61	1.588.76	1.553.80	2.347.99	2.331.70
2	166	0.54	290	21868	1856.57	1794.79	1.856.58	1.794.79	2.338.94	2.252.25
3	371	0.82	73	23178	2089.32	1906.47	2.089.33	1.906.47	2.342.16	2.233.58
4	488	1	66	26408	2074.04	?	2.074.04	2.033.88	2.344.87	2.236.40
5	969	1.06	52	31156	2176.52	2196.54	2.176.53	2.144.43	2.329.25	2.231.52
6	1052	1.05	63	35310	2330.90	2141.93	2.181.75	2.141.93	2.325.25	2.211.70
7	1861	0.88	39	19100	2263.89	2235.67	2.263.89	2.235.67	2.309.80	2.246.50
8	1503	0.79	56	13794	2269.59	2358.18	2.269.60	2.228.63	2.336.83	2.280.35
9	2292	0.58	69	13446	2305.06	2285.08	2.305.07	2.285.08	2.316.45	2.275.70
10	2277	0.51	103	9766	2330.41	2343.38	2.330.41	2.278.93	2.322.56	2.291.65
11	2311	0.44	213	17770	2349.49	2346.81	2.349.49	2.255.58	2.319.60	2.285.75
12	2037	0.36	178	9144	2303.18	2287.97	2.303.19	2.287.97	2.329.24	2.298.20

Calc. $p\text{CO}_2$ (μatm)	TPC		PIC		POC		Chl <i>a</i>		POC:PON	PIC:POC
	content (pg C cell $^{-1}$)	Prod. (pg C cell $^{-1}$ d $^{-1}$)	content (pg C cell $^{-1}$)	Prod. (pg C cell $^{-1}$ d $^{-1}$)	content (pg C cell $^{-1}$)	Prod. (pg C cell $^{-1}$ d $^{-1}$)	content (pg C cell $^{-1}$)	Prod. (pg C cell $^{-1}$ d $^{-1}$)		
50	41.99	12.18	22.75	6.60	19.24	5.58	0.20	0.06	4.06	1.18
166	36.16	25.31	25.10	13.37	11.41	10.46	0.21	0.12	5.57	2.20
371	44.84	26.50	29.98	24.58	14.86	10.90	0.28	0.23	3.76	2.02
488	40.37	27.20	26.03	26.03	14.34	11.37	0.24	0.24	6.55	1.81
969	31.29	24.07	19.81	21.00	11.48	10.33	0.22	0.23	6.09	1.73
1052	31.43	21.52	19.29	20.26	12.13	9.32	0.22	0.23	6.08	1.59
1861	41.35	19.94	22.39	19.71	18.95	8.68	0.26	0.22	6.96	1.18
1503	37.50	19.03	20.11	15.88	17.39	8.22	0.21	0.16	5.93	1.16
2292	30.93	17.79	15.50	8.99	15.44	7.51	0.14	0.08	5.50	1.00
2277	31.86	16.86	15.87	8.09	15.99	6.94	0.15	0.08	5.81	0.99
2311	29.84	16.68	13.64	6.00	16.20	6.72	0.12	0.05	5.86	0.84
2037	42.75	16.16	21.55	7.76	21.20	6.41	0.16	0.06	5.69	1.02

AIII
15°C

Bottle #	calculated $p\text{CO}_2$ (μatm)	μ (cell d^{-1})	Cell densities		uncorrected DIC ($\mu\text{mol kg}^{-1}$)		corrected DIC ($\mu\text{mol kg}^{-1}$)		TA ($\mu\text{mol kg}^{-1}$)	
			initial	final	initial	final	initial	final	initial	final
1	44	0.13	429	10064	1593.98	1848.6	1593.98	1582.93	2344.86	2316.27
2	102	0.41	165	21954	1798.62	1862.84	1798.63	1732.90	2343.50	2259.76
3	216	0.61	288	37200	1932.0	1908.45	1932.07	1908.45	2327.52	2223.74
4	290	0.66	129	13308	2037.76	1987.95	2037.76	1987.95	2338.17	2288.69
5	476	0.62	245	9987	2111.58	2055.47	2111.59	2055.47	2297.16	2272.37
6	599	0.57	135	13462	2221.77	2085.03	2177.28	2085.03	2321.77	2268.85
7	1133	0.44	90	18518	2249.76	2245.48	2249.77	2184.12	2314.12	2259.26
8	1165	0.33	54	14730	2289.92	2208.6	2251.60	2208.60	2317.19	2276.59
9	1663	0.25	397	10900	2286.02	2254.41	2286.03	2254.41	2298.58	2280.46
10	1276	0.35	201	18414	2308.42	2261.37	2308.43	2261.37	2369.01	2316.22
11	1421	0.39	222	33876	2343.12	2419.13	2343.13	2299.05	2410.77	2320.84
12	2774	0.13	300	7362	2348.81	2368.15	2348.81	2316.32	2286.45	2275.63

calculate d $p\text{CO}_2$ (μatm)	TPC		PIC		POC		Chl <i>a</i>		POC:PON	PIC:POC
	content (pg C cell $^{-1}$)	Prod. (pg C cell $^{-1}$ d $^{-1}$)	content (pg C cell $^{-1}$)	Prod. (pg C cell $^{-1}$ d $^{-1}$)	content (pg C cell $^{-1}$)	Prod. (pg C cell $^{-1}$ d $^{-1}$)	content (pg C cell $^{-1}$)	Prod. (pg C cell $^{-1}$ d $^{-1}$)		
44	41.79	5.43308	28.56	3.71	13.23	1.72	0.12	0.02	5.68	2.16
102	36.22	14.8514	25.69	10.53	10.53	4.32	0.14	0.06	6.84	2.44
216	28.47	17.3651	19.15	11.68	9.32	5.68	0.12	0.07	6.44	2.05
290	36.31	23.9653	23.86	15.75	12.45	8.22	0.15	0.10	6.95	1.92
476	38.66	23.9697	23.30	14.45	15.36	9.52	0.16	0.10	5.97	1.52
599	35.58	20.2826	21.45	12.23	14.13	8.05	0.15	0.09	6.78	1.52
1133	36.66	16.1291	21.25	9.35	15.40	6.78	0.13	0.06	6.63	1.38
1165	33.46	11.0419	18.09	5.97	15.37	5.07	0.12	0.04	6.57	1.18
1663	39.04	9.75987	17.63	4.41	21.41	5.35	0.10	0.02	6.19	0.82
1276	33.64	11.7727	12.68	4.44	20.95	7.33	0.12	0.04	6.60	0.61
1421	33.35	13.0083	22.04	8.60	11.31	4.41	0.11	0.04	6.64	1.95
2774	43.39	5.64115	20.75	2.70	22.65	2.94	0.08	0.01	6.64	0.92

NOTE: numbers marked red in “uncorrected initial and final DIC” column are the individual values which were not use and later calculated from TPC in “corrected initial and final DIC”.

AIV. Carbonate system parameters calculated from measured TA and DIC averages.

20 °C						15 °C					
calc. $p\text{CO}_2$ (μatm)	CO_3^{2-} ($\mu\text{mol kg}^{-1}$)	HCO_3^- ($\mu\text{mol kg}^{-1}$)	CO_2^* ($\mu\text{mol kg}^{-1}$)	$\Omega\text{-Ca}$	pH_{total}	calc. $p\text{CO}_2$ (μatm)	CO_3^{2-} ($\mu\text{mol kg}^{-1}$)	HCO_3^- ($\mu\text{mol kg}^{-1}$)	CO_2^* ($\mu\text{mol kg}^{-1}$)	$\Omega\text{-Ca}$	pH_{total}
50	524.20	1045.50	1.60	12.54	8.71	44	504.52	1082.28	1.65	12.03	8.76
166	325.00	495.30	5.40	7.77	8.34	102	365.96	1396.00	3.79	8.72	8.51
371	206.50	1779.40	12.00	4.94	8.07	216	245.53	1666.66	8.05	5.85	8.26
488	172.60	1865.60	15.80	4.13	7.97	290	211.34	1790.70	10.80	5.03	8.17
969	102.50	2026.70	31.30	2.45	7.71	476	147.45	1918.30	17.77	3.51	7.98
1052	95.00	2032.90	34.00	2.27	7.68	599	125.41	1983.39	22.33	2.98	7.89
1861	59.00	2130.70	60.10	1.41	7.45	1133	74.28	2100.36	42.29	1.77	7.64
1503	72.80	2127.70	48.60	1.74	7.54	1165	73.17	2113.45	43.47	1.74	7.63
2292	49.70	2171.30	74.00	1.19	7.37	1663	53.29	2154.86	62.05	1.27	7.49
2277	50.50	2180.60	73.50	1.21	7.37	1276	70.23	2167.04	47.62	1.67	7.60
2311	49.60	2178.30	74.60	1.19	7.36	1421	65.18	2202.88	53.02	1.55	7.57
2037	56.10	2173.70	65.80	1.34	7.42	2774	33.16	2195.85	103.53	0.79	7.27

AV. Nutrient concentrations at beginning and end of experiment

20 °C	final **	
pCO ₂	PO ₄ ³⁻ (μmol kg ⁻¹)	NO ₃ ⁻ (μmol kg ⁻¹)
50	7.27	56.55
166	6.62	61.17
371	6.43	60.99
488	6.13	56.61
969	6.05	61.86
1052	5.89	64.74
1861	5.93	62.67
1503	5.99	61.24
2292	5.86	65.18
2277	5.81	70.49
2311	5.33	66.61
2037	5.53	69.55

15 °C	initial *		final **	
pCO ₂	PO ₄ ³⁻ (μmol kg ⁻¹)	NO ₃ ⁻ (μmol kg ⁻¹)	PO ₄ ³⁻ (μmol kg ⁻¹)	NO ₃ ⁻ (μmol kg ⁻¹)
44	4.05	57.28	3.80	58.11
102	4.05	57.28	3.67	60.28
216	4.05	57.28	3.06	53.50
290	4.05	57.28	3.59	59.32
476	4.05	57.28	3.08	56.01
599	4.05	57.28	3.26	62.91
1133	4.05	57.28	2.78	58.49
1165	4.05	57.28	3.17	66.22
1663	4.05	57.28	2.62	60.06
1276	4.05	57.28	3.16	65.47
1421	4.05	57.28	3.03	66.88
2774	4.05	57.28	2.92	69.11

* From 50 L ASW stock

** From individual (2 L) bottles at end of experiment

NOTE: no data for initial nutrient concentrations at 20 °C due to loss of samples

Appendix VI. POP and PON content and production rates

20°C	POP		PON	
$p\text{CO}_2$	content ($\mu\text{g POP cell}^{-1}$)	production ($\mu\text{g POP cell}^{-1} \text{d}^{-1}$)	content (pg N cell^{-1})	production ($\text{pg N cell}^{-1} \text{d}^{-1}$)
50	3.11	0.90	4.74	1.38
166	0.82	0.44	2.05	1.11
371	0.76	0.63	3.96	3.24
488	0.85	0.85	2.19	2.19
969	0.74	0.78	1.88	2.00
1052	0.77	0.81	2.00	2.10
1861	1.48	1.30	2.72	2.40
1503	1.83	1.45	2.93	2.32
2292	2.01	1.16	2.81	1.63
2277	2.88	1.47	2.75	1.40
2311	2.16	0.95	2.76	1.22
2037	4.18	1.50	3.73	1.34

15°C	POP		PON	
$p\text{CO}_2$	content ($\mu\text{g POP cell}^{-1}$)	production ($\mu\text{g POP cell}^{-1} \text{d}^{-1}$)	content (pg N cell^{-1})	production ($\text{pg N cell}^{-1} \text{d}^{-1}$)
44	1.61	0.21	2.33	0.30
102	0.96	0.40	1.54	0.63
216	0.65	0.40	1.45	0.88
290	1.50	0.99	1.79	1.18
476	2.08	1.29	2.57	1.59
599	1.80	1.03	2.08	1.19
1133	1.72	0.76	2.32	1.02
1165	1.74	0.57	2.34	0.77
1663	3.48	0.87	3.46	0.87
1276	1.98	0.69	3.17	1.11
1421	1.25	0.49	1.70	0.66
2774	5.08	0.66	3.41	0.44

Literature

Bach, L. Calcification and photosynthesis of the coccolithophore *Emiliana huxleyi* cultured under a broad range of carbonate chemistry conditions. Kiel University, Diploma Thesis (2009)

Balch W.M., Holligan P.M., Ackleson S.G. Voss K.J. Biological and optical properties of mesoscale coccolithophore blooms in the Gulf of Maine. *Limnology and Oceanography* 36, 629-643 (1991)

Balch W.M., Holligan P.M., Kilpatrick K.A. Calcification, photosynthesis and growth of the bloom-forming coccolithophore, *Emiliana huxleyi*. *Continental Shelf Research* 12, 1353-1374 (1992)

Balch, W and Kilpatrick K. Calcification rates in the equatorial Pacific along 140 W. *Deep-Sea Research* 43, 971-993 (1996)

Balch, W., Drapeau D.T., Fritz J.J. Monsoonal forcing of calcification in the Arabian Sea. *Deep-Sea Research* 47, 1301-1337(2000)

Balch W., Drapeau D., Bowler B., Booth E. Prediction of pelagic calcification rates using satellite measurements. *Deep-Sea Research* 54, 478-495 (2007)

Barker S., Hoggings J., Elderfield H. The future of the carbon cycle: review, calcification response, ballast and feedback on atmospheric CO₂. *Philosophical Transactions of the Royal Society* 361, 1977-1999 (2003)

Billet D.S.M., Lampitt R.S., Rice A.L., Mantoura R.F.C. Seasonal sedimentation of phytoplankton to the deep-sea benthos. *Nature* 302, 520-522 (1983)

Bollman J., Klaas C. Morphological variation of *Gephyrocapsa oceanica* Kamptern 1943 in Plankton samples: implications for ecologic and taxonomic interpretations. *Protist* 159, 369-381 (2008)

Bouman H., Platt T., Sathyendranath S., Li W., Stuart V., Fuentess-Yaco C., Maass H., Horne E., Ulloa O., Lutz V., Kyewalayanga M. Temperature as indicator of optical properties and community structure of marine phytoplankton: implications for remote sensing. *Marine Ecology Progress Series* 258, 19-30 (2003)

Broerse A.T.C., Brummer G.J., Van Hinte J.E. Coccolithophore export production in response to monsoonal upwelling off Somalia (northwestern Indian ocean). *Deep Sea Research* 47, 2179-2205 (2000)

Broerse A.T.C., Tyrrell T., Young J.R., Poulton A.J., Merico A., Balch W.M., Miller P.I. The cause of bright waters in the Bering Sea in winter. *Continental Shelf Research* 23, 1579-1596 (2003)

Buesseler K.O., Lamborg C.H., Boyd P.W., Lam P.J., Trull T.W., Bidigare R.R., Bishop J.K.B., Casciotti K.L., Dehairs F., Elskens M., Honda M., Karl D.M., Siegel D.A., Silver M.W., Steinberg D.K., Valdes J., Van Mooy B., Wilson S. Revisiting Carbon flux through the Ocean's twilight zone. *Science* 316, 567-570 (2007)

Buitenhuis E.T., Van der Wal P., de Baar H.J.W. Blooms of *Emiliana huxleyi* are sinks of atmospheric Carbon Dioxide: A field and Mesocosm study derived Simulation. *Global Biochemical Cycles* 15, 577-587 (2001)

Buitenhuis E., Pangerc T., Franklin D., Le Quere C., Malin G. Growth rates of six coccolithophorid strains as a function of temperature. *Limnology and Oceanography* 53, 1181-1185 (2008)

Caldeira K., Wickett M. Anthropogenic carbon and ocean pH. *Nature* 425, 365 (2003)

Carder K.L., Lee Z.P., Hawes S.K., Kamykowski D. Semianalytic moderate-resolution imaging spectrometer algorithms for chlorophyll a and absorption with bio-optical domains based on nitrate-depletion temperatures. *Journal of Geophysical Research Oceans* 104, 5403-5421 (1999)

Colmenero-Hidalgo E., Flores J., Sierro F.J., Barcena M.A., Lowemark L., Schonfeld J., Grimalt J.O. Ocean surface water response to short-term climate changes revealed by coccolithophores from the Gulf of Cadiz (NE Atlantic) and Alboran Sea (W Mediterranean). *Palaeogeography, Paleoclimatology, Palaeocology* 205, 317-336 (2004)

Conte M., Thompson A., Lesley D., Harris R. *Geochimica et cosmochimica acta* 62, 51-68 (1998)

Danbara A., Shiraiwa Y. The requirement for Selenium for the growth of marine coccolithophorids, *Emiliana huxleyi*, *Gephyrocapsa oceanica* and *Helladosphaera* sp (Prymnesiophyceae). *Plant and Cell Physiology* 40, 762-766 (1999)

De Bernardi B., Ziveri P., Erba E., Thunell R.C. Coccolithophore export production during the 1997-1998 El Nino event in Santa Barbara Basin (California). *Marine Micropaleontology* 55, 107-125 (2005)

De Bodt C., Van Oostende N., Harlay J., Sabbe K., Chou L. Individual and interacting effect of $p\text{CO}_2$ and temperature on *Emiliana huxleyi* calcification: study of the calcite production, the coccolith morphology and the coccosphere size. *Biogeosciences* 7, 1401-1412 (2010)

Delille B., Harlay J., Zondervan I., Jacquet S., Chou L., Wollast R., Bellerby R., Frankignoulle M., Borges A., Riebesell U., Gattuso J.P. Global biogeochemical cycles 19 (2005)

- Dickson A., Sabine C., Christian J. Guide to best practices for ocean CO₂ measurements. Sydney, British Columbia. North Pacific Marine Science Organization, PICES Special publication (2007)
- Doney S., Fabry V., Feely R., Kleypas JA. Ocean acidification: the other CO₂ problem. Annual Review of Marine Sciences 1, 162-192 (2009)
- Engel A., Zondervan I., Aerts K., Beaufort L., Benthien A., Chou L., Delille B., Gattuso J.P., Harlay J., Heeman C., Hoffmann L., Jacquet S., Nejstgaard J., Pizay D., Newall E., Schneider U., Terbruggen A., Riebesell U. Testing the direct effect of CO₂ concentration on a bloom of the coccolithophore *Emiliania huxleyi* in mesocosm experiments. Limnology and Oceanography 50, 493-507 (2005)
- Feng Y., Warner M., Zhang Y., Sun J., Fu F., Rose J., Hutchins A. Interactive effects of increased pCO₂, temperature and irradiance on the marine coccolithophore *Emiliania huxleyi* (Prymnesiophyceae). European Journal of Phycology 43, 87-89 (2008)
- Frankignoulle M., Canon C., Gattuso J.P. Marine calcification as a source of carbon dioxide: positive feedback of increasing atmospheric CO₂. Limnology and Oceanography 39, 458-462 (1994)
- Gage J.D., Tyler P.A. Deep-sea Biology. Cambridge University Press (1991)
- Gangsto R., Gehlen M., Schneider B., Bopp L., Aumont O., Joos F. Modeling the marine aragonite cycle: changes under rising carbon dioxide and its role in shallow water CaCO₃ dissolution. Biogeosciences discussions 5, 1655-1687 (2008)
- Gehlen M., Gangsto R., Schneider B., Bopp L., Aumont O., Ethe C. The fate of pelagic CaCO₃ production in a high CO₂ ocean: a model study. Biogeosciences 4, 505-519 (2007)
- Gooday A. Biological responses to seasonally varying fluxes of organic matter to the ocean floor: a review. Journal of Oceanography 58, 305-332 (2002)
- Groom S.B., Holligan P.M. Remote sensing of Coccolithophore blooms. Advanced Space Research 7, 73-78 (1987)
- Hansen H.P., Koroloeff F. Determination of nutrients. In: Grasshoff, K., Kremling K., Ehrhardt M. Methods of Seawater analysis, 159-228 (1999)
- Holligan P.M., Viollier M., Harbour D.S., Camus P., Champagne-Phillippe M. Satellite and ship studies of coccolithophore production along a continental shelf edge. Nature 304, 339-342 (1983)

Holligan P.M., Fernandez E., Balch W.M., Boyd P., Burkill P., Finch M., Groom S.B., Malin G., Muller K., Purdie D.A., Robinson C., Trees C.C., Turner S.M., Van Der Wal P. A Biogeochemical Study of the Coccolithophore, *Emiliana Huxleyi*, in the North Atlantic, *Global Biogeochem. Cycles*, 7(4), 879–900 (1993)

Iglesias-Rodriguez M.D., Halloran P.R., Rickaby R.E.M., Hall I.R., Colmenero-Hidalgo E., Gittins J.R., Green D.R.H., Tyrrell T., Gibbs S.J., Von Dassow P., Rehm E., Armbrust E.V., Boessenkool K.P. Phytoplankton calcification in a high-CO₂ world. *Science* 320, 336-340 (2008)

Jackson R., Carpenter S., Dahm C., McKnight D., Niaman R., Postel S., Running S. Water in a changing world. *Ecological Applications* 11, 1027-1045 (2008)

Jasper J.P., Hayes J.M. A carbon isotope record of CO₂ levels during the late Quaternary. *Nature* 347, 462-464 (1990)

Jasper J.P., Hayes J.M., Mix A.C., Prahl F.G. Photosynthetic fractionation of ¹³C and concentrations of dissolved CO₂ in the central equatorial Pacific during the last 255,000 years. *Paleoceanography* 9, 781-798 (1994)

Jin X., Gruber N., Dunne J., Sarmiento J., Armstrong R. Diagnosing the contribution of phytoplankton functional groups to the production and export of particulate organic carbon, CaCO₃, and opal from global nutrient and alkalinity distributions. *Global Biogeochemical Cycles* 20 (2006)

Joos F., Plattner G., Stocker T., Marchal O., Schmittner A. Global warming and marine carbon cycle feedbacks on future atmospheric CO₂. *Science* 284, 464-467 (1999)

Kester D., Duedall I., Connors D., Pytkowicz R. Preparation of Artificial Seawater. *Limnology and Oceanography* 12, 176-179 (1967)

Klass C., Archer D.E. Association of sinking organic matter with various types of mineral ballast in the deep sea: Implications for the rain ratio. *Global Biochemical Cycles* 5 (2002)

Kleypas et al. The future of coral reefs in an age of global change. *Int. J Earth Sciences* 90, 426-437 (2001)

Knappertsbusch M., Brummer J.A. A sediment trap investigation of sinking coccolithophorids in the North Atlantic. *Deep Sea Research Part I: Oceanographic Research Papers* 42, 1083-1109 (1995)

Langer G., Geisen M., Bauman K., Kläs J., Riebesell U., Thoms S., Young J. Strain-specific responses of calcifying algae to changin seawater carbonate chermistry. *Geochemistry, gephysics, geosystems* 7 (2006)

- Langer G., Nehrke G., Probert I., Ly J., Ziveri P. Strain-specific responses of *Emiliana huxleyi* to changing seawater carbonate chemistry. *Biogeosciences Discussions* 6, 4361-4383 (2009)
- Levitus S., Antonov J., Boyer T. Warming of the world oceans, 1955-2003. *Geophysical Research Letters* 32 (2005)
- Maier-Reimer E., Mikolajewicz U., Winguth A. Future ocean uptake of CO₂: interaction between ocean circulation and biology. *Climate Dynamics* 12, 711-721 (1996)
- Marsh, M.E. Regulation of CaCO₃ formation in coccolithophores. *Comparative Biochemistry and Physiology Part B* 136, 743-754 (2003)
- Matebr R., Hirst A. Climate change feedback on the future oceanic CO₂ uptake. *Tellus* 51, 722-733 (1999)
- McIntyre A., Be A. Modern coccolithophoridae of the Atlantic ocean-I: placoliths and Cyrtoliths. *Deep-sea Research* 14, 561-597 (1967)
- Nanninga HJ and Tyrrell T. The importance of light for the formation of algal blooms by *Emiliana huxleyi*. *Marine Ecology Progress Series*, 136: 195-203 (1996)
- Nissuma A., Pesant S., Bellerby R.G.J, Delille B, Middelburg J., Orr J., Riebesell U., Tyrrell T., Wolf-Gladrow D., Gattuso J.P. Earth system science data discussions 3, 109-130 (2010)
- Orr J.C., Fabry V.J., Aumont O., Bopp L., Doney S.C., Feely R.A., Gnanadesikan A., Gruber N., Ishida A., Joos F., Key R.M., Lindsay K., Maier-Reimer E., Matear R., Monfray P., Mouchet A., Najjar R.G., Plattner G., Rodgers K.B., Sabine C.L., Sarmiento J.L., Schlitzer R., Slater R.D., Totterdell I.J., Weirig M., Yamanaka Y., Yool A. Anthropogenic ocean acidification over twenty-first century and its impact on calcifying organisms. *Nature* 437, 681-686 (2005)
- Petit J.R. Jouzel J., Raynaud D., Barkov N., Barnola J.M., Basile I., Benders M., Chappellaz J., Davis M., Delaygue G., Delmotte M., Kotlyakov V.M., Legrand M., Lipenkov V.Y., Lorius C., Pepin L., Ritz C., Saltzman E., Stievenard M. Climate and atmospheric history of the past 420,000 years from the Vostok ice core, Antarctica. *Nature* 399, 429-436 (1999)
- Plattner G.K., Joos F., Stocker T.F., Marchal O. Feedback mechanisms and sensitivities of ocean carbon uptake under global warming. *Tellus* 53, 564-592 (2003)
- Prahl F.G., Muehlhausen L.A., Zahnle D.L. Further evaluation of long-chain alkenones as indicators of paleoceanographic conditions. *Geochimica et Cosmochimica* 52, 2303-2310 (1988)

Revelle R., Suess H. Carbon dioxide exchange between atmosphere and ocean and the question of an increase in atmospheric CO₂ during past decades. *Tellus IX* (1957)

Reynaud S., Leclercq N., Romaine_Lioud S., Ferrier-Pages C., Jaubert J., Gattuso J. Interacting effects of CO₂ partial pressure and temperature on photosynthesis and calcification in scleractinian coral. *Global Change Biology* 9, 1660-1668 (2003)

Rickaby R.E.M., Hendriks J., Young J.N. Perturbing phytoplankton: a tale of isotopic fractionation in two coccolithophore species. *Climate of the Past Discussions* 6, 257-294 (2010)

Ridgwell A., Zondervan I., Hargreaves J.C., Bijma J., Lenton T.M. Assessing potential long-term increase of oceanic fossil fuel CO₂ uptake due to CO₂-calcification feedback. *Biogeosciences* 4, 481-492 (2007)

Ridgwell A., Schmidt D.N., Turley C., Brownlee C., Maldonado M.T., Tortell P., Young J.R. From laboratory manipulations to Earth system models: scaling calcification impacts of ocean acidification. *Biogeosciences* 6, 2611-2623 (2009)

Riebesell U., Zondervan I., Rost B., Tortell P.D., Zeebe R.E., Morel F.M.M. Reduced calcification of marine plankton in response to increased atmospheric CO₂. *Nature* 407, 364-367 (2000)

Riebesell U., Körtzinger A., Oschlies A. Sensitivities of marine carbon fluxes to ocean change. *Proceedings of the National Academy of Sciences* 106 (2009)

Rohdes L., Peake B., Mackenzie A., Marwick S. *New Zealand journal of marine and freshwater research* 29, 345-357 (2009)

Rohdes L., Peake B., MacKenzie L., Marwick S. Coccolithophores *Gephyrocapsa oceanica* and *Emiliana huxleyi* (Prymnesiophyceae = Haptophyceae) in New Zealand's coastal waters: characteristics of blooms and growth in laboratory culture. *New Zealand Journal of Marine and Freshwater Research* 29, 345-357 (1995)

Rost B., Zondervan I., Wolf-Gladrow D. Sensitivity of phytoplankton to future changes in ocean carbonate chemistry: current knowledge, contradictions and research directions. *Marine Ecology Progress Series* 373, 227-237 (2008)

Ryther J.H., Guillard R.R.L. Studies of marine planktonic diatoms: II use of *Cyclotella nana hustedt* for assays of vitamin B₁₂ in seawater. *Canadian Journal in Microbiology* 8, 437-445 (1962)

Sabine C.L., Feely R.A., Gruber N., Key R.M., Lee K., Bullister J.L., Wanninkhof R., Wong C.S., Wallace D.W.R., Tilbrook B., Millero F.J., Peng T., Kozyr A., Ono T., Rios A.F. The Oceanic Sink for Anthropogenic CO₂. *Science* 305, 367-371 (2004)

Samtleben C., Bickert T. Coccoliths in sediment traps from the Norwegian Sea. *Marine Micropaleontology* 16, 39-64 (1990)

Sarmiento J., LeQuere C. Oceanic carbon dioxide uptake in a model of century-scale global warming. *Science* 274, 1346-1350 (1996)

Sarmiento J., Dunne J., Gnanadesikan A., Key R., Matsumoto K., Slater R. A new estimate of the CaCO_3 to organic carbon export ratio. *Global Biogeochemical Cycles* 16 (2002)

Sarmiento J.L., Slater R., Barber R., Bopp L., Doney S.C., Hirst A.C., Kleypas J., Matear R., Mikolajewicz U., Monfray P., Soldatov V., Spall S.A., Stouffer R. Response of ocean ecosystems to climate warming. *Global Biochemical Cycles* 18 (2004)

Sarmiento J.L., Gruber N. *Ocean biogeochemical dynamics*. Princeton University Press, Princeton USA (2006)

Sathyendranath S., Cota G., Stuart V., Maass H., Platt T. Remote sensing of phytoplankton pigments: a comparison of empirical and theoretical approaches. *International Journal of Remote Sensing* 22, 249-273 (2001)

Schiebel R. Planktonic foraminiferal sedimentation and the marine calcite budget. *Global Biogeochemical Cycles* 16, 1-21 (2002)

Schmittner A., Oschlies A., Matthews H., Galbraith E. Future changes in climate, ocean circulation, ecosystems and biogeochemical cycling simulated for a business-as-usual CO_2 emission scenario until year 4000 AD. *Global Biogeochemical Cycles* 22 (2008)

Schulz K., Barcelos e Ramos J., Zeebe R.R., Riebesell U. CO_2 perturbation experiments: similarities and differences between dissolved inorganic carbon and total alkalinity manipulations. *Biogeosciences* 6, 2145-2153 (2009)

Sharp J.H. Improved analysis for "particulate" organic carbon and nitrogen from seawater. *Limnology and Oceanography* 19, 984-989 (1974)

Shi D., Xu Y., Morel F.M.M. Effects of the pH/ pCO_2 control method on medium chemistry and phytoplankton growth. *Biogeosciences* 6, 1199-1207 (2009)

Stoll H.M., Bakker K., Nobbe G.H., Haese R.R. Continuous flow analysis of dissolved inorganic carbon content in seawater. *Analytical chemistry* 73, 4111-4116 (2001)

Stoll H.M., Ziveri P. Separation of monospecific and restricted coccolith assemblages from sediments using differential settling velocity. *Marine Micropaleontology* 46, 209-221 (2002)

- Stoll H.M., Ziveri P. Coccolithophorid-based geochemical properties. Coccolithophores- from molecular processes to global impact. Springer, New York (2004)
- Tyrell T., Taylor A.H. A modelling study of *Emiliana huxleyi* in the NE Atlantic. J. of Marine Systems 9, 83-112 (1996)
- Volkman J.K., Barrett S.M., Blackburn S.I., Sikes E.L. Alkenones in *Gephyrocapsa oceanica*: Implications of studies of paleoclimate. Geochimica et Cosmochimica Acta 59, 513-520 (1995)
- Welschmeyer N.A. Fluorimetric analysis of chlorophyll a in the presence of chlorophyll b and pheopigments. Limnology and Oceanography 39, 1985-1992 (1994)
- Winter A., Jordan R.W., Roth P.H. Biogeography of living coccolithophores in ocean waters. Cambridge University Press, New York USA (1994)
- Wohlers J., Engel A., Zöllner E., Breithaupt P., Jürgens K., Hoppe H., Sommer U., Riebesell U. Changes in biogenic carbon flow in response to sea surface warming. Proceedings of the National Academy of Sciences (2009)
- Wolf-Gladrow D., Riebesell U., Burkhardt S. Bijma J. Direct effects of CO₂ concentration on growth and isotopic composition of marine plankton. Tellus 51B, 461-476 (1999)
- Wolf-Gladrow D., Zeebe R., Klaas C., Körtzinger A., Dickson A. Total alkalinity: the explicit conservative expression and its application to biogeochemical processes. Marine Chemistry 106, 287-300 (2007)
- Ziveri P., Thunell R.C., Domenico R. Export production of coccolithophores in an upwelling region: Results from San Pedro Basin, Southern California borderlands. Marine Micropaleontology 24, 335-358 (1995)
- Ziveri P and Broerse A. Sedimentation of Coccolithophores in the North Atlantic ocean (48N,21W). The Oceanography Society Meeting (1996)
- Ziveri P., Bernardi B., Baumann K., Stoll H., Mortyn P. Sinking of coccolith carbonate and potential contribution to organic carbon ballasting in the deep ocean. Deep Sea Research 54, 659-675 (2007)
- Zondervan I., Zeebe R.E., Rost B., Riebesell U. Decreasing marine biogenic calcification: A negative feedback on rising atmospheric pCO₂. Global Biogeochemical Cycles 15, 507-516 (2001)
- Zondervan I., Rost B., Riebesell U., Effect of CO₂ concentration on the PIC/POC ratio in the coccolithophore *Emiliana huxleyi* grown under light-limiting conditions and different day lengths. J. of Experimental Marine Biology and Ecology 272, 55-70 (2002)

Acknowledgments

To my advisor Ulf Riebesell for being a great role model as a scientist, teacher and individual. Thank you for letting me be part of your group for this project.

Special thanks to my supervisor, friend and teacher Kai Schulz for always having the time to explain (patiently) all mathematical, theoretical and non-scientific questions I had and for gracefully filling all my drafts with helpful comments and feedback. I complain all the time but I really appreciate it.

Many thanks to Mario Lebrato for surviving after reading the first drafts of the thesis and always contributing to new ideas and information.

Thanks to room 324 (aka Jasmin, Lennart and Sarah) for always having the door open for me to bother with non-scientific issues and for being such incredible role models as young scientists. You guys rock!

Thanks to my office-mates: Antje, Jan and Luke for always asking about my progress and helping in any way they could.

To Andrea, Kerstin and Peter for giving me all the knowledge I needed to carry all my laboratory methods/work as efficiently as possible.

To my friends and family for always having positive reinforcement when I was frustrated and smiling-politely while I talked about ocean acidification and coccolithophores (even when they didn't understand), thank you anyways.

To all the people I forgot to mention, thank you for being part of this journey.

Last but not least, to my parents for always encouraging me to follow my dreams, to fight for what I wanted and for giving me the opportunity to fly away from home to achieve that. I sacrificed our time together but I know you are proud of me, thank you forever for all the financial and emotional support. To Tefi and Roberto, for being two of the greatest inspirations in my life and for giving me a reason to be better each day. I love you both. There will never be enough words to thank you.

Declaration on Oath

I hereby certify that this work entitled "The combined effect of global warming and ocean acidification on the coccolithophore *Gephyrocapsa oceanica* carbon production and physiology" was completely and solely written by me without any other sources or help than the ones mentioned. I also confirm that this work has never been submitted to other higher education institutions.

I declare myself in agreement that this Master thesis is forwarded to the libraries of the IFM-GEOMAR and the Christian-Albrechts Universität zu Kiel. I certify that the digital copy of this Master thesis is the same as the printed version.

Scarlett Sett

August 11th 2010